"One has to realize that the experimental and theoretical understanding of nuclear reactions is one of the major achievements of Nuclear Physics of the last half century, largely unrecognized or celebrated, even by nuclear physicists themselves" (H. Feshbach)

Nuclear reactions:

- development of collision theory
- conservation of mass

(http://www.theo.phys.ulg.ac.be)

Ecole Joliot-Curie 2007

J. CUGNON, ULg

Nuclear Reactions. A short digest.

- Generalities
- Typical variations & first classification
- Coherent reactions
- Incoherent (high energy) reactions
- Reactions involving coherent & incoherent effects
- Specific features linked to particular projectiles
- Outlook

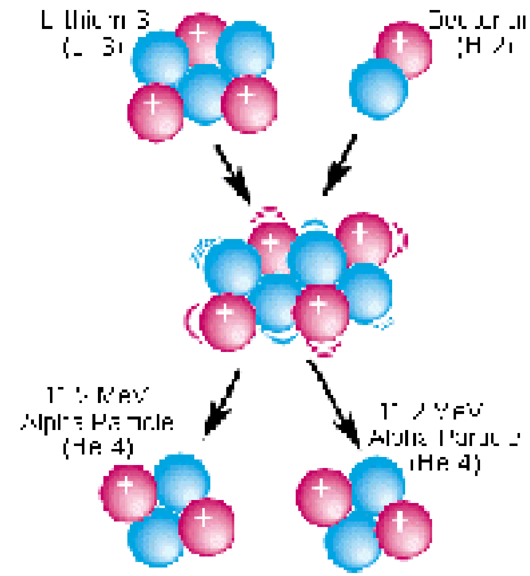

Lithium-6 - Deuterium Reaction

1. Introduction

- Experiment

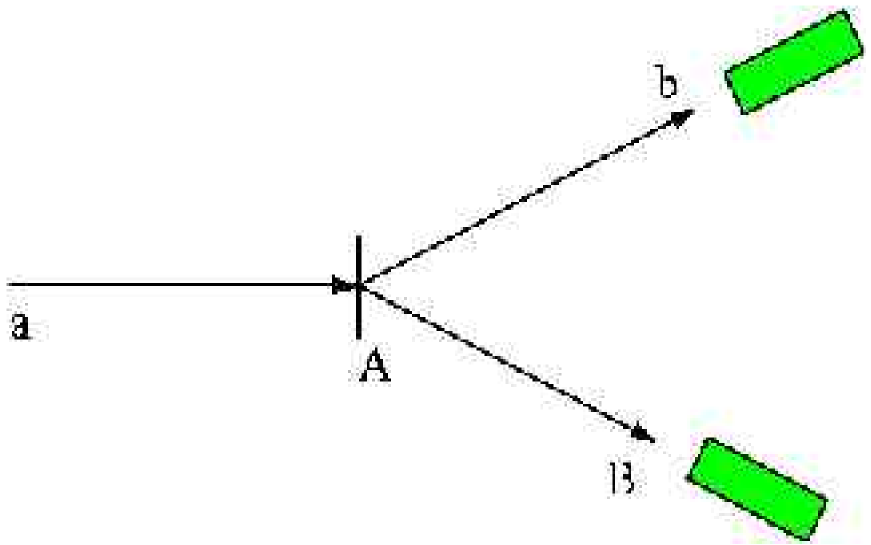

- Control parameters: *a, A,* E_{inc}*, (ΔE, polarisations, ...)*

- Detection ⇨ asymptotic states only

$$a+A \rightarrow b_1+b_2^*+...+[\pi,\gamma,..]$$

- if only b_1 is detected: *inclusive* reactions $a+A \rightarrow b_1+X$
- if all are detected: *exclusive* reactions
- intermediate: *semi-inclusive* reactions

- Information is encoded in (differential) cross-sections

- Standard theoretical description

$$\chi_c = \psi_p \psi_t e^{i\vec{k}_c.\vec{r}_c} \quad \rightarrow \quad \chi_c' = \psi_{f_1} \psi_{f_2} \ldots e^{i\vec{k}_c'.\vec{r}_c'} \ldots$$

$$H = H_0 + V$$

$$T = V + V \frac{1}{E - H + i\varepsilon} V$$

$$E = \frac{\hbar^2 k_c^2}{2m} + E_i = \frac{\hbar^2 k_{c'}^2}{2m} + E_f = \frac{\hbar^2 k_{c'}^2}{2m} + E_i - Q$$

interaction

structure

$$d\sigma_{cc'} = \frac{(2\pi)^4}{\hbar v_c} \delta\left(\frac{\hbar^2 k_c^2}{2m} + E_i - \frac{\hbar^2 k_{c'}^2}{2m} - E_f\right) \left| \langle f \vec{k}_c' | T | i \vec{k}_c \rangle \right|^2 d\omega$$

- calculation of cross-sections = formidable task
- connection with structure is not obvious
- reaction mechanism

d.o.f —*hypotheses* / *approximations*→ reaction model (mechanism) → structure

- there exist time-dependent approaches

$$\frac{\partial \rho}{\partial t} = -\frac{i}{\hbar}\left[H , \rho\right]$$

$$\left[\frac{\partial}{\partial t} + \frac{\vec{p}}{m}.\vec{\nabla} - (\vec{\nabla} U).\vec{\nabla}_p\right] f(\vec{r}, \vec{p}, t) = I_{coll}[f]$$

INC, BUU, LV, QMD...

macroscopic properties

symmetries:

(a) *time-reversal invariance* $\Rightarrow$ detailed balance

$$\langle i -\vec{k}_c | T | f -\vec{k}_c{}' \rangle = \langle f\, \vec{k}_c{}' | T | i\, \vec{k}_c \rangle \qquad k_c^2 \frac{d\sigma_{cc'}}{d\Omega}(\Omega) = k_{c'}^2 \frac{d\sigma_{c'c}}{d\Omega}(-\Omega)$$

simplifies if angular momentum is disregarded:

$$S_{c'c} = \delta_{c'c} - 2 i \pi \left(\frac{m^2 k_c k_{c'}}{2\pi} \right)^{1/2} \langle f\, \vec{k}_c{}' | T | i\, \vec{k}_c \rangle$$ does not depend upon angle

$$\sigma_{cc'} = \pi \lambda_c^2 \left| S_{c'c} - \delta_{c'c} \right|^2 \qquad S_{cc'} = S_{c'c}^{*}$$

(b) *conservation of norm*

$$S^{+} S = 1 \qquad \sum_{c'} \left| S_{c'c} \right|^2 = 1 \qquad \sigma_c^T = 2\pi \lambda_c^2 (1 - \Re S_{cc}) \qquad \sigma_c^T = -\frac{4\pi}{k_c} \Im f_{cc}$$

(c) *conservation of angular momentum, isospin, etc*

➔ specificity of typical reactions

2. Variation of cross-sections with control parameters

A. Characteristic variations

Behaviour close to threshold:

1. channel without Coulomb interaction (incident neutrons)

elastic scattering $\sigma_{cc} \approx C$

endothermic reaction Q<0 $\sigma_{cc'} \approx C\sqrt{E-E_{th}}$

exothermic reaction Q>0 $\sigma_{cc'} \approx C/k_{c'}$

2. reactions with Coulomb interaction

elastic scattering may be dominated by Coulomb scattering

reaction: multiplication with Gamow factor $G_c = \exp\left(-\frac{Z_1 Z_2 e^2}{\hbar v_c}\right)$

3. total reaction cross-section $\approx \pi R^2 \approx$ 1b @ high energy

Typical energy dependences

n-induced exothermic reaction

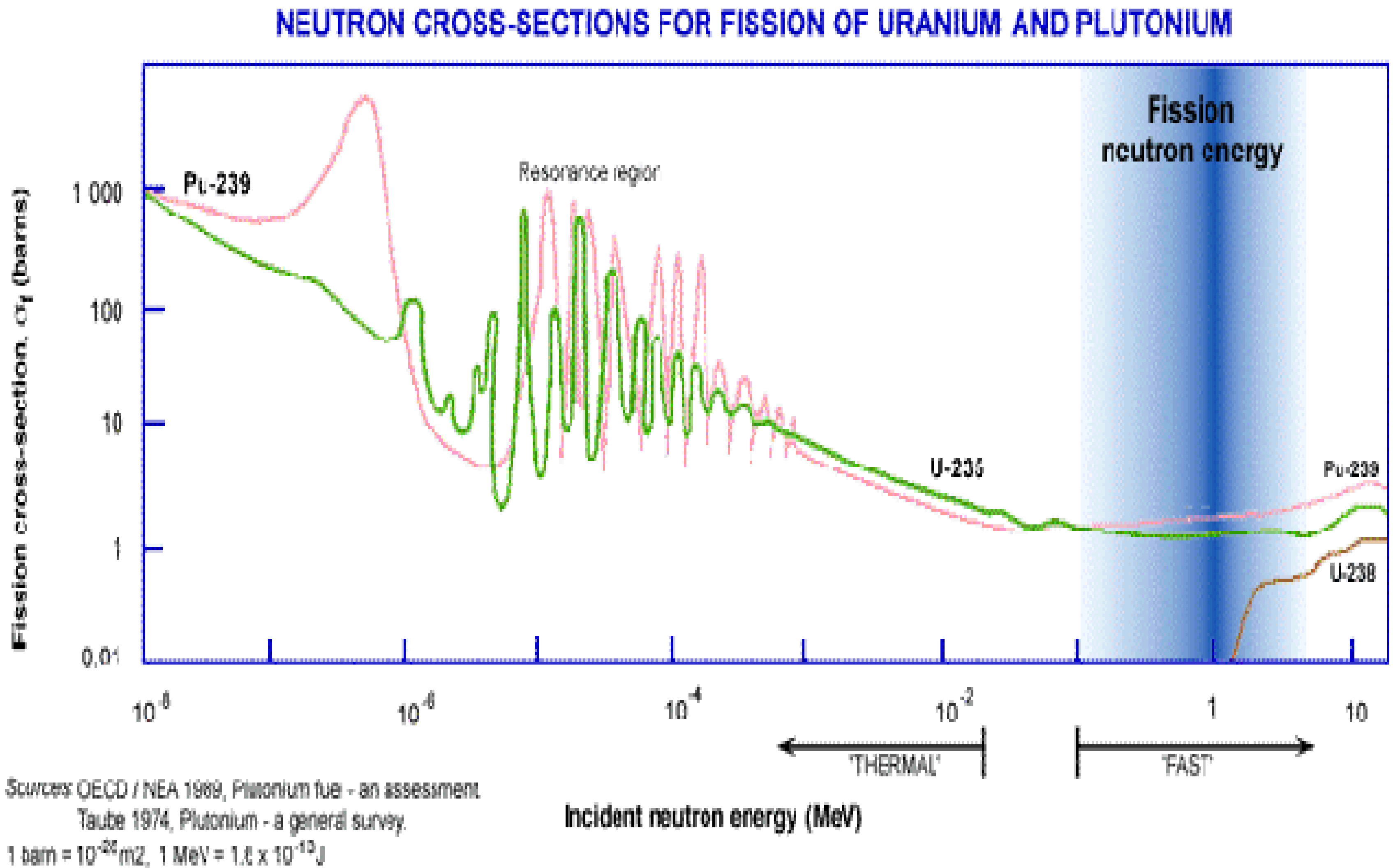

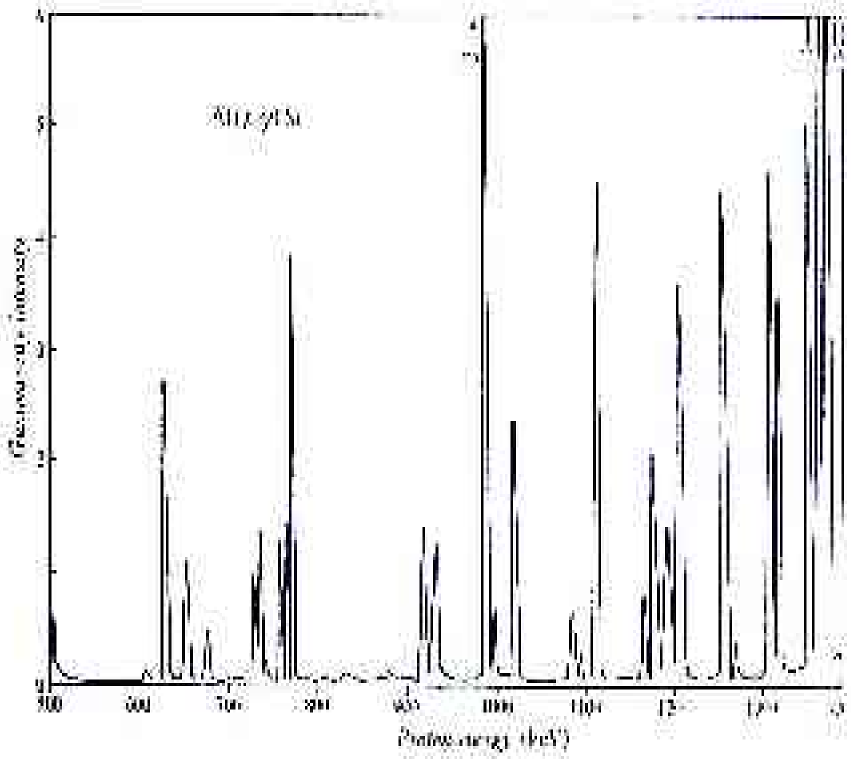

Fig. 15.4 Resonant yield of γ-radiation in the reaction $^{27}Al(p,\gamma)Si^{28}$. The peaks indicate virtual levels at an excitation of about 12 MeV in the nucleus ^{28}Si (Brostrom et al., *Phys. Rev.*, 71, 661, 1947).

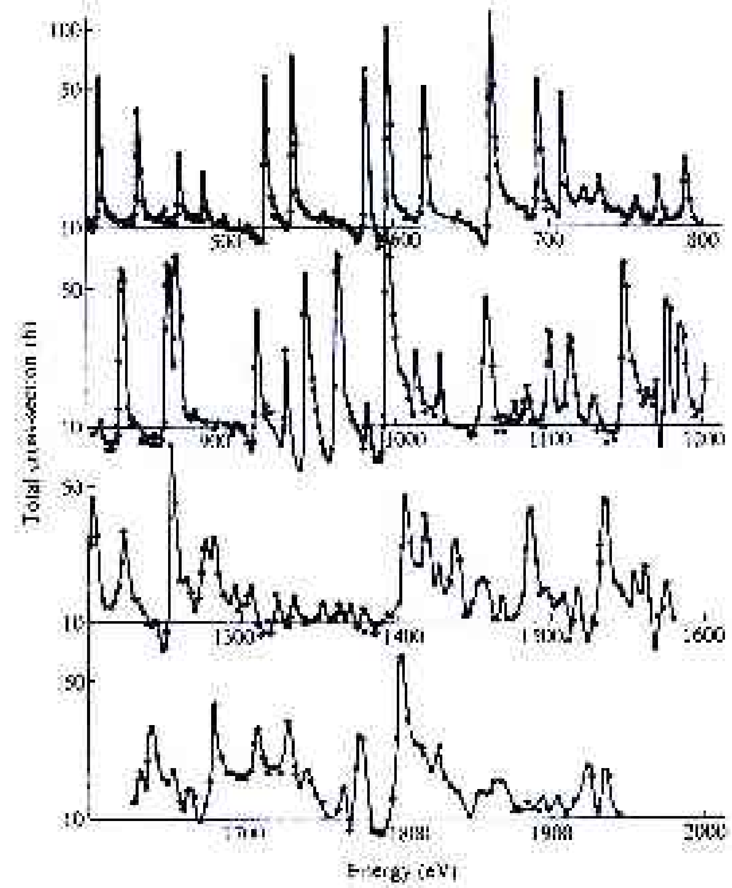

Fig. 1.1 Resonances in low-energy neutron scattering (Firk et al. 1960).

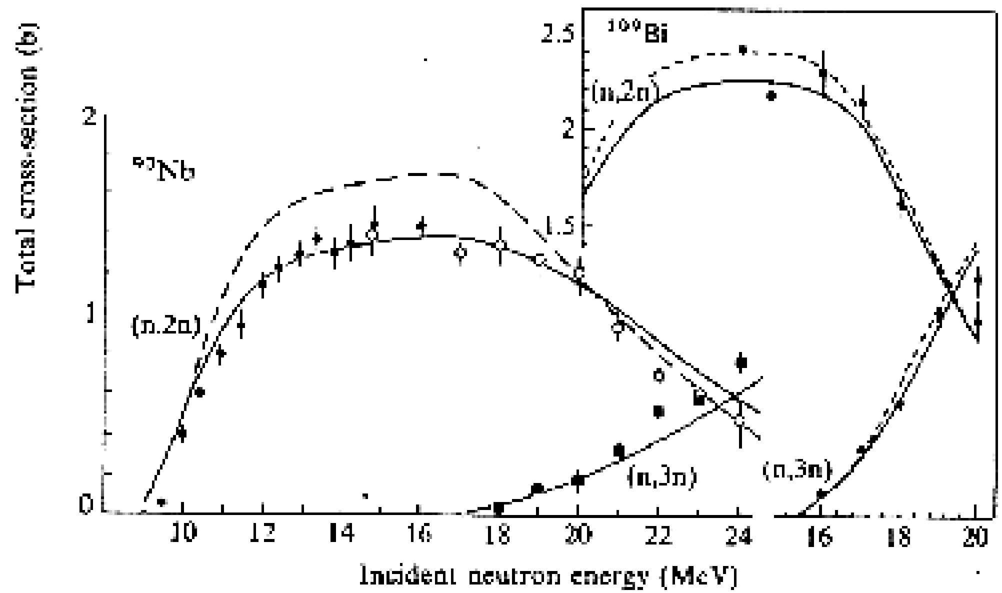

Total cross-section (b)
93Nb
209Bi
(n,2n)
(n,2n)
(n,3n)
(n,3n)
Incident neutron energy (MeV)

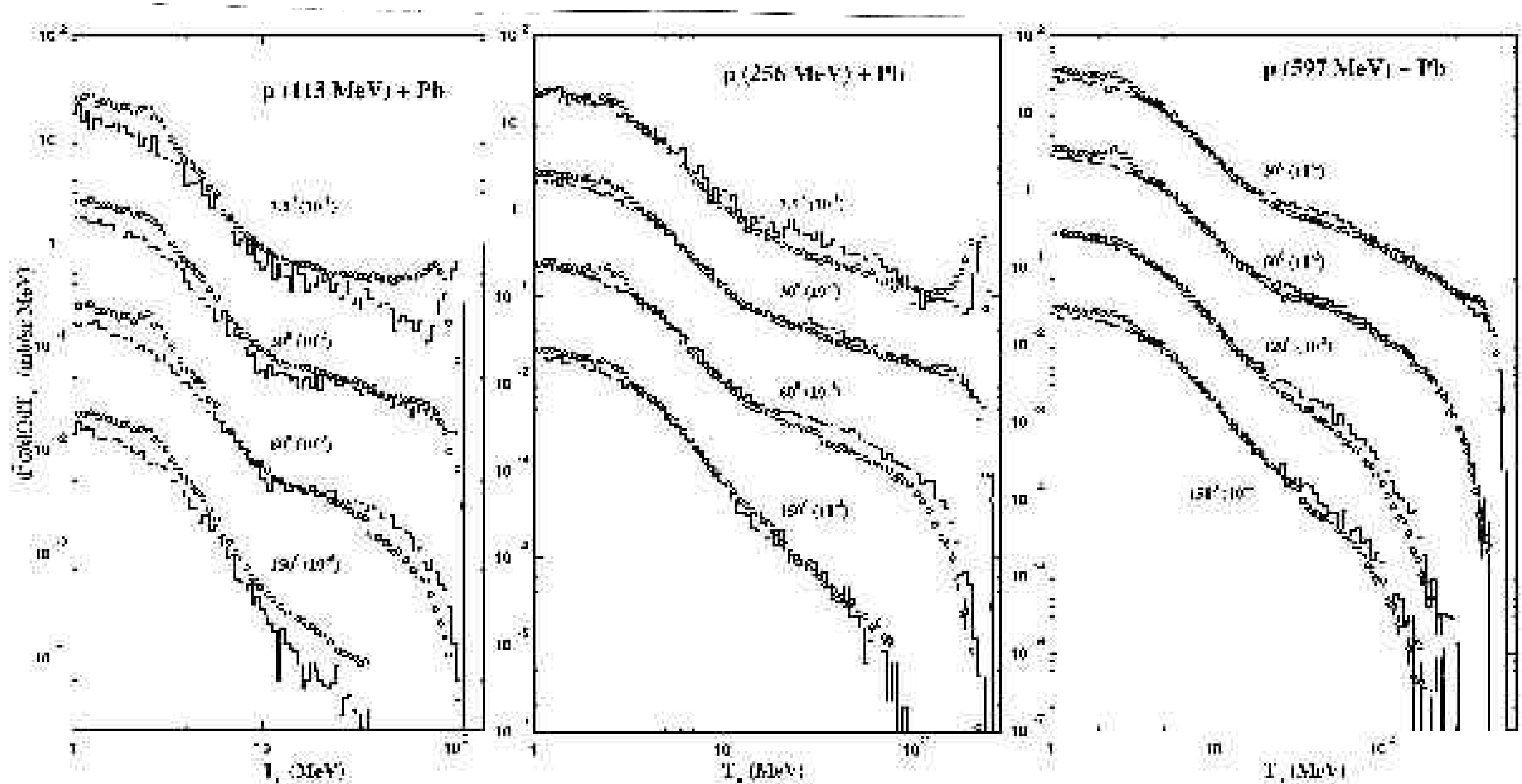

p (113 MeV) + Pb
p (256 MeV) + Pb
p (597 MeV) + Pb

Typical target dependences

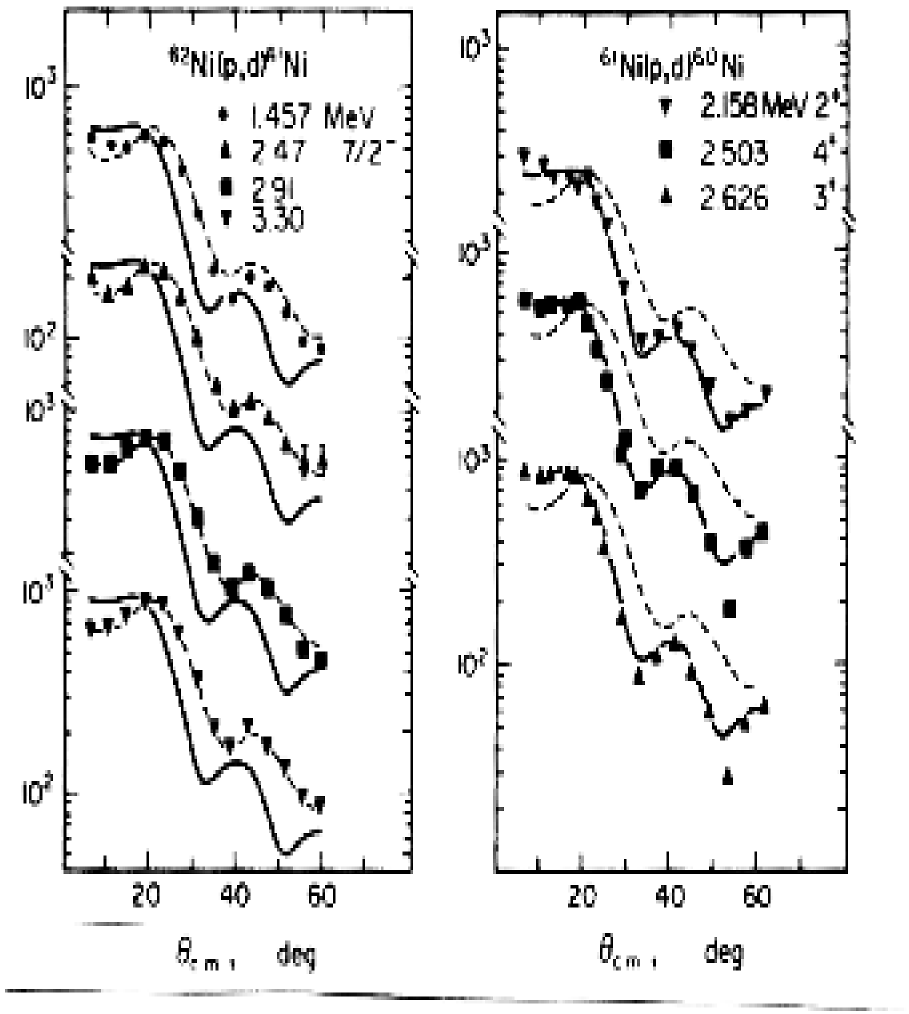

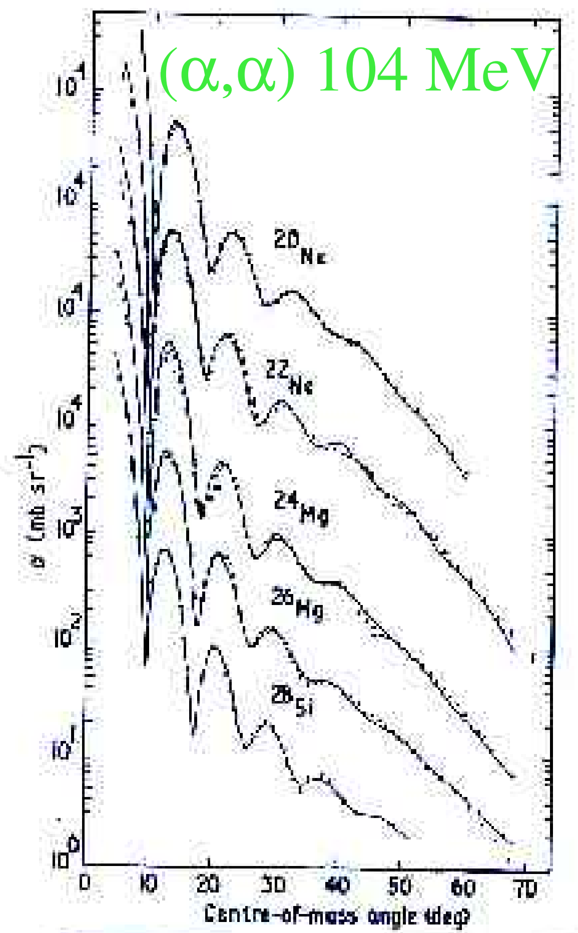

B. Comparison of control parameters with typical lengths and energies

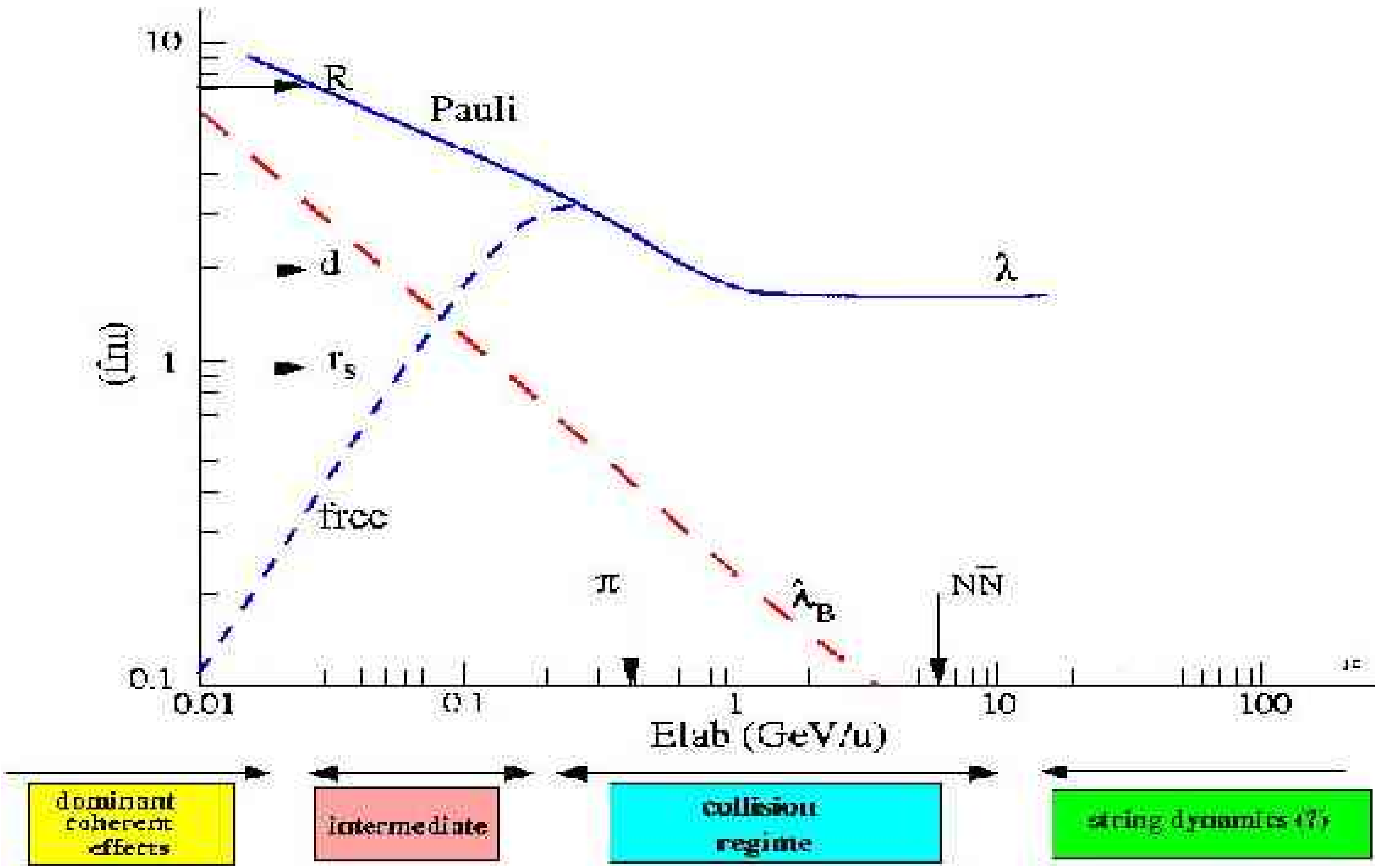

!: mixing of regimes due to the impact ("uncontrolled") parameter

First "rough" classification

1. Quantum treatment is needed → wave function related information
   - elastic &slightly inelastic collisions
   - resonant reactions
   - pick-up & transfert reactions

2. Quasi-classical treatment is (perhaps) sufficient → more global properties
   - (moderately) inelastic collisions
   - fragmentation (spallation) collisions

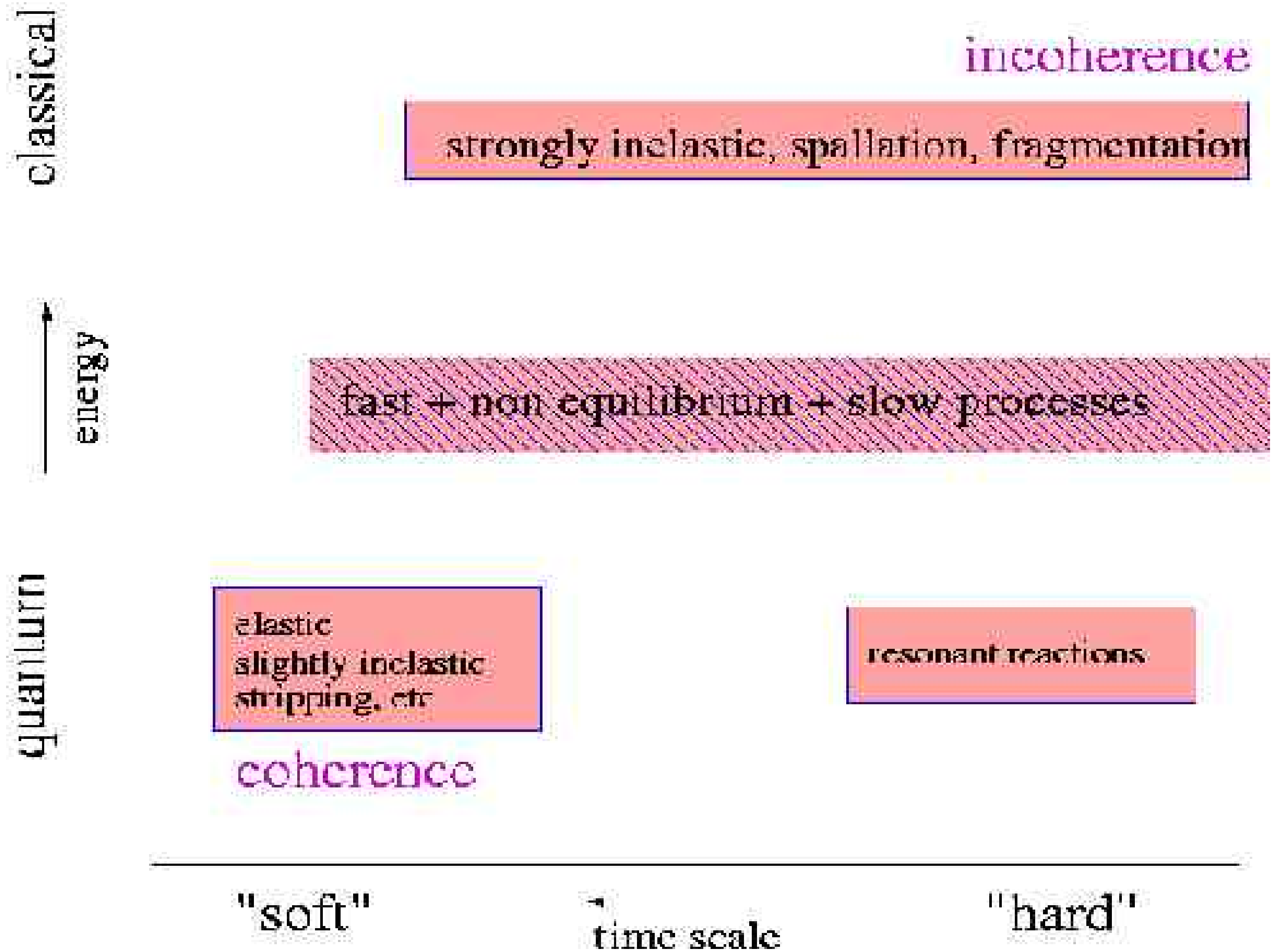

classical
incoherence
strongly inelastic, spallation, fragmentation
energy
fast + non equilibrium + slow processes
quantum
elastic
slightly inelastic
stripping, etc
resonant reactions
coherence
"soft"
time scale
"hard"

C. Comparison nucleon-nucleus ⇔nucleus-nucleus

1. *Differences linked with the shape of the colliding system*
   - deep inelastic collisions
   - fusion reactions & partial fusion reactions

2. *Differences linked with the number of particles*
   - thermodynamic properties of nuclear matter
   - possible phase transition (multifragmentation)

3. Coherent, quasi-coherent & resonant reactions

A. Resonant reactions. The compound nucleus.

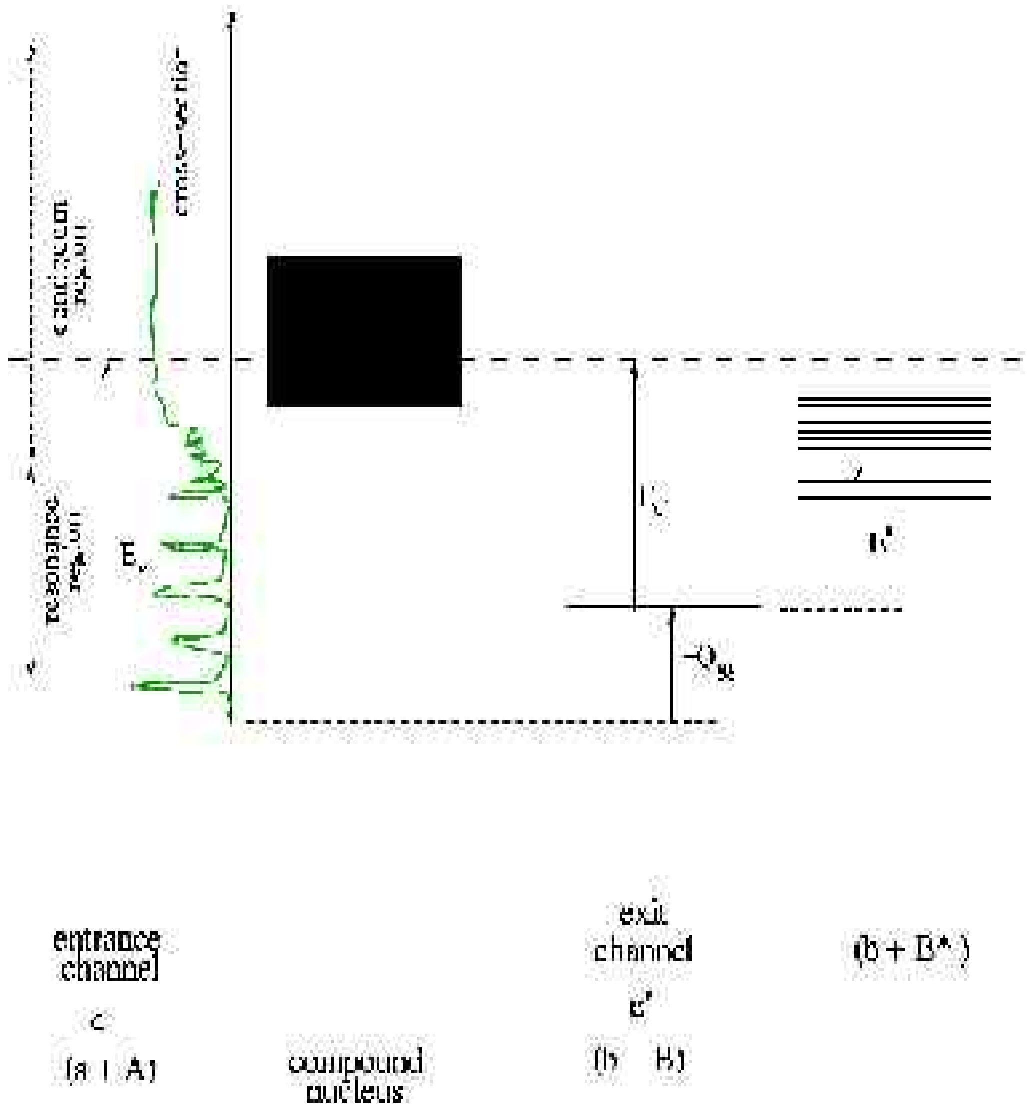

☛resonance ⇒"definite" energy with lifetime $\tau=\hbar/\Delta E \gg t_{pass}=R/v$

☛Bohr' hypothesis:
formation of a complex CN state,
followed by a statistical decay in open channels

☛formation & decay are independent, except for conservation laws
⇒ symmetric angular distributions (around 90°)

The Breit-Wigner formula

S-matrix form

$$S_{cc'} = e^{i(\delta_c + \delta_{c'})}\left(\delta_{cc'} - i\sum_\lambda \frac{\omega_\lambda}{E - E_\lambda + i\Gamma_\lambda/2}\right) \qquad \sigma_{cc'} = \pi \lambdabar_c^2 \left|S_{cc'} - \delta_{cc'}\right|^2$$

Bohr Hypothesis $\quad \omega_\lambda = \Gamma_{\lambda c}^{1/2}\Gamma_{\lambda c'}^{1/2}, \quad \sum_c \Gamma_{\lambda c} = \Gamma_\lambda, \quad (\Gamma_{\lambda c}^{1/2} = real)$

$$\sigma_{cc'} = \sigma_c^{CN} P_{c'}$$

with

$$\sigma_c^{CN} = \pi \lambdabar_c^2 \frac{\Gamma_{\lambda c}\Gamma_\lambda}{(E - E_\lambda)^2 + \Gamma_\lambda^2/4}, \qquad P_{c'} = \frac{\Gamma_{\lambda c'}}{\Gamma_\lambda}$$

Structure Information (SI): E_λ, (J^π), Γ_λ, $\Gamma_{\lambda c}$

The shell-model approach

$$H = H_0 + V = \sum_i h_0(i) + V \qquad H_0 \varphi_i = E_i \varphi_i, \quad H_0 \chi_c(E) = E \chi_c(E)$$

$$\Psi_c^+ = \sum_i b_i(E) \varphi_i + \sum_{c'} a_c^{c'}(E) \chi_{c'}(E)$$

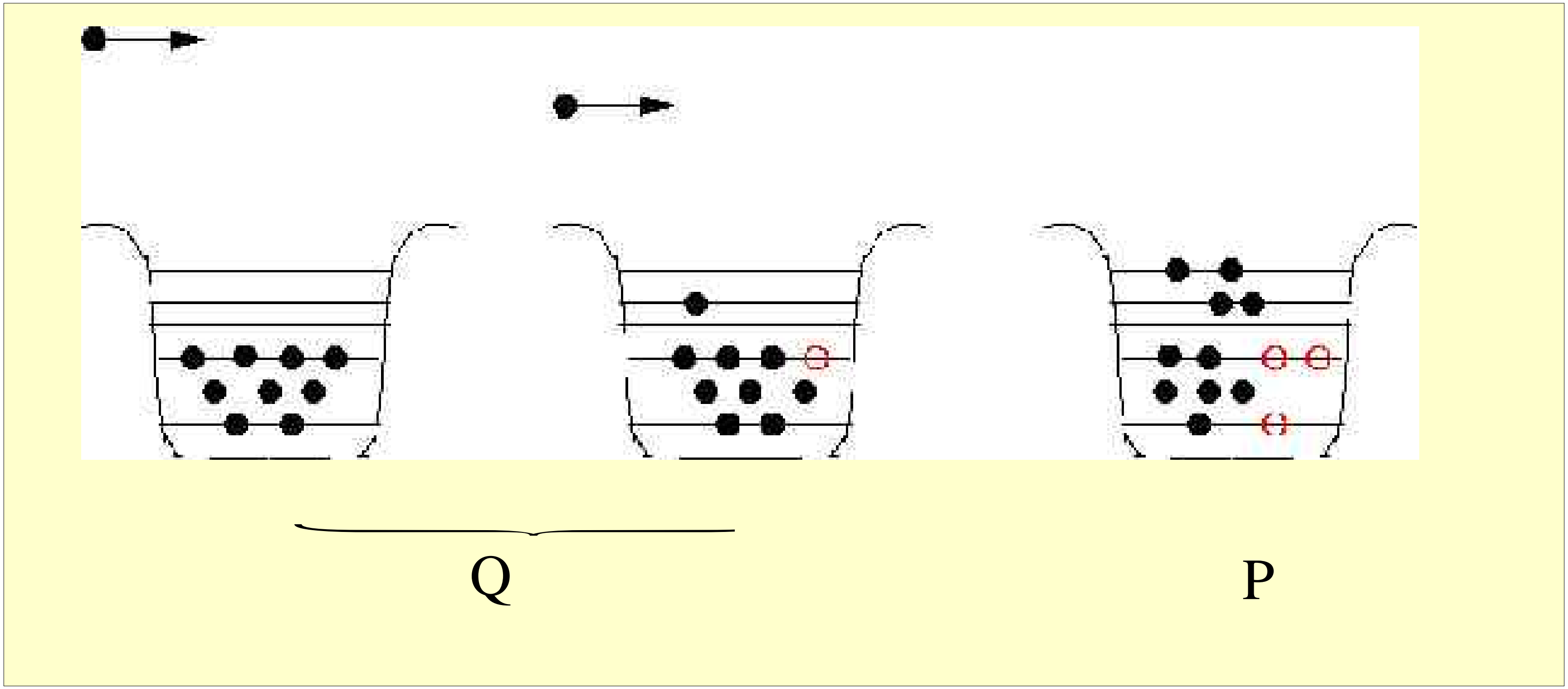

in absence of direct coupling $<\chi_c|V|\chi_{c'}>=0$:

$$S_{cc'}=e^{i(\delta_c+\delta_{c'})}\left[\delta_{cc'}-i2\pi\sum_j \frac{\langle\chi_c|V|\Phi_j\rangle\langle\Phi_j|V|\chi_{c'}\rangle}{E-E_j-i\pi\sum_{c^+}\left|\langle\Phi_j|V|\chi_c\rangle\right|^2}\right]$$

Note that Φ_j are (complicated) eigenstates of

$[PHP + PVQ\,(E-H_0)^{-1}\,QVP]\Phi_j = E_j\,\Phi_j$

They are *bound states in the continuum* (E>0)

Also: continuum component in loosely bound states

$\Gamma_{\lambda c}=\pi\left|\langle\chi_c|V|\Phi_\lambda\rangle\right|^2$ represents the coupling of the resonant states to channel c

Average cross-sections and the overlapping resonance region

NB: no average for overlapping resonances

$$\left\langle \sigma_{cc'} \right\rangle = \frac{1}{I} \int_{E-I/2}^{E+I/2} \pi \lambda_c^2 \left| \sum_\lambda \frac{\Gamma_{\lambda c}^{1/2} \Gamma_{\lambda c'}^{1/2}}{E - E_\lambda + i\Gamma_\lambda/2} \right|^2 dE$$

$$\approx \frac{1}{I} \int_{E-I/2}^{E+I/2} \pi \lambda_c^2 \sum_\lambda \frac{\Gamma_{\lambda c} \Gamma_{\lambda c'}}{(E - E_\lambda)^2 + \Gamma_\lambda^2/4} dE$$

$$= \pi \lambda_c^2 \frac{2\pi}{D} \overline{\left(\frac{\Gamma_{\lambda c} \Gamma_{\lambda c'}}{\Gamma_\lambda} \right)}$$

Hauser-Feshbach formula:

$$\left\langle \sigma_{cc'} \right\rangle = \pi \lambda_c^2 \frac{\left(\frac{2\pi}{D} \overline{\Gamma_{\lambda c}} \right)\left(\frac{2\pi}{D} \overline{\Gamma_{\lambda c'}} \right)}{\frac{2\pi}{D} \overline{\Gamma_\lambda}} F_{cc'} = \pi \lambda_c^2 \frac{T_c T_{c'}}{\sum_c T_c} F_{cc'}$$

F accounts for width correlations

B. Elastic scattering. The optical model

The *optical model:* elastic scattering can be reduced to potential scattering

$$V_{opt}(r) \approx -V_0 \frac{\rho(r)}{\rho_0} + V_{LS} - i\,W(r) = V_C + V_{LS}$$

W>0 accounts for the loss of flux (above the 1st inelastic channel)

Two theories:

1. elimination of the inelastic components

$$(E-PHP)P\Psi = PHQ\,Q\Psi\,, \quad (E-QHQ)Q\Psi = QHP\,P\Psi \rightarrow E-PHP-PHQ(E+i\varepsilon-QHQ)^{-1}QHP\,P\Psi=0$$

2. mass operator

They predict V_{opt} to be energy-dependent and non-local

JLM microscopic potential

$$V_C(E,\vec{r}) = \int d^3\vec{r}\,' G(E', \rho(\vec{r}\,'))\, f(\vec{r} - \vec{r}\,')$$

G is the Brueckner G-matrix

Phenomenological potentials

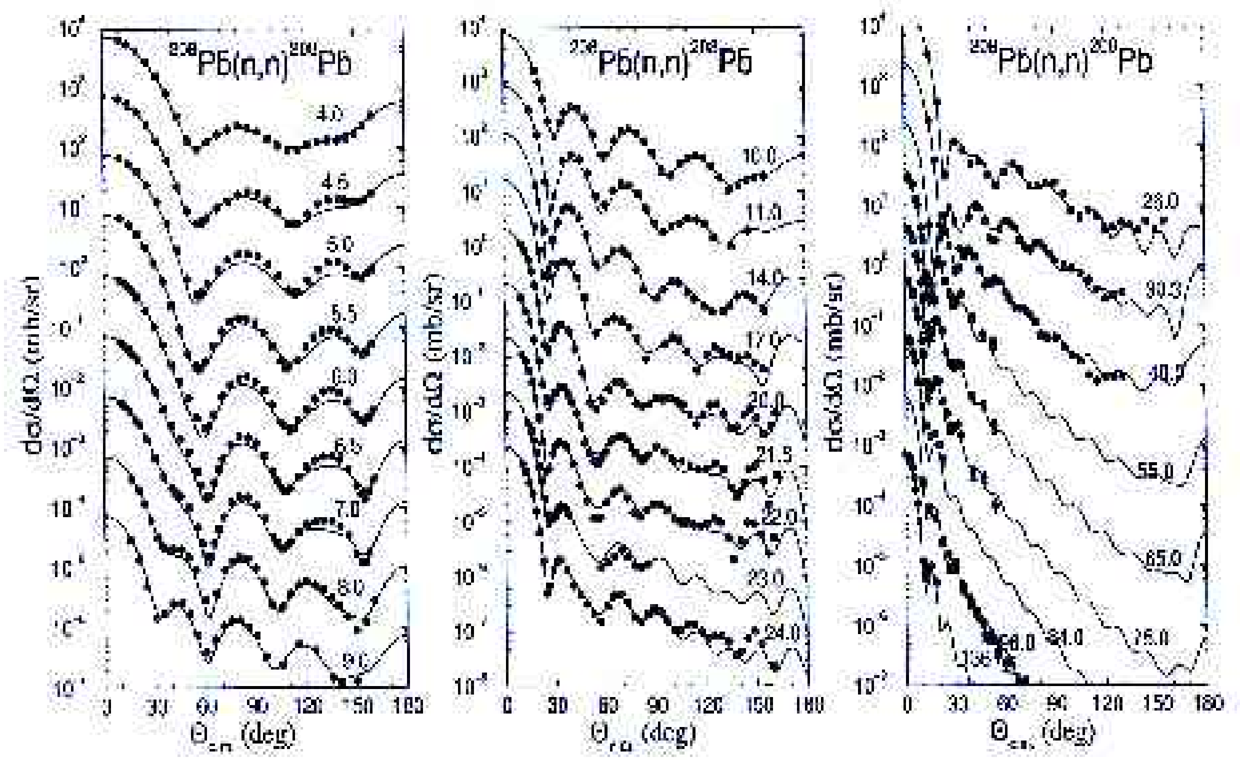

- Parameters are smoothly dependent upon the target
- The crucial "parameter" is the volume integral of the central part

$$J = \int V_C(r)\, d^3\vec{r}$$

- Largely diffractive scattering

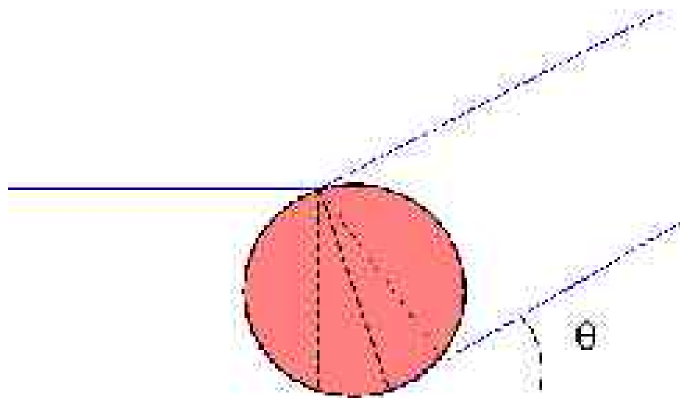

maxima @ 2kRsin $\theta/2 = n\pi$

- Structure Information (SI): geometry, deformation
- relativistic formulation is better for spin-orbit part
- OM -> $\langle S_{cc} \rangle = e^{i2\delta c}(1-\Gamma_{\lambda c}/D)$

$OMP \Rightarrow T_c \Rightarrow$ (HF) average cross-sections

C. Inelastic scattering. (p,p')

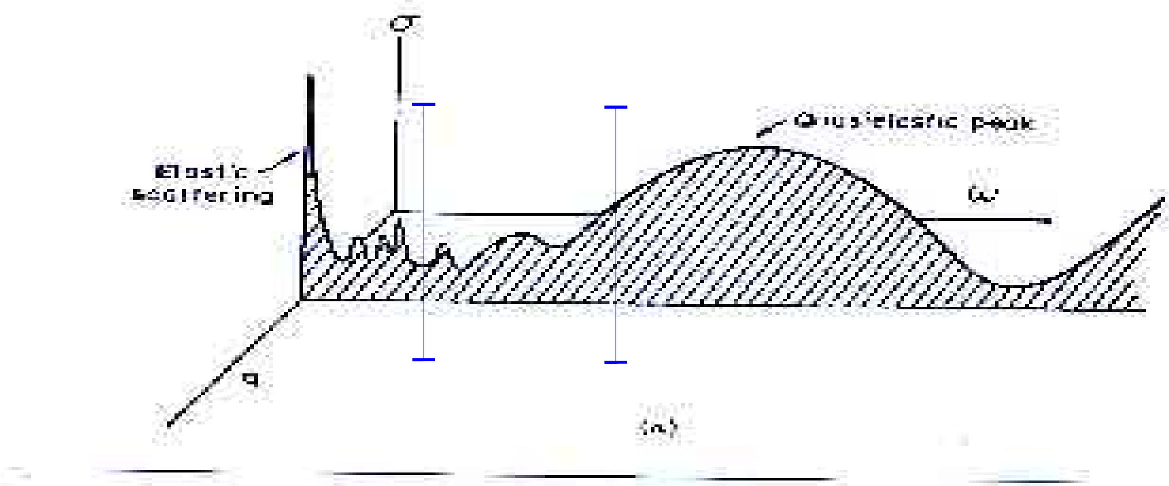

SI: Energy levels

Direct interactions: only one NN interaction

Distorted wave Born approximation (DWBA) Born: T="V"

$$\frac{d\sigma}{d\Omega} \propto \left| \left\langle \chi_{c'}(\vec{r})\Phi_{c'} \left| \sum_i v(\vec{r}-\vec{r}_i) \right| \chi_c(\vec{r})\Phi_c \right\rangle \right|^2 \rightarrow \propto \left| \left\langle \Phi_{c'} \left| \sum_i e^{-i\vec{q}.\vec{r}_i} \right| \Phi_c \right\rangle \right|^2 = \left| e^{-i\vec{q}.\vec{r}} \rho_{cc'}(\vec{r}) \right|^2$$

SI: transition form factors ->w.f.

$$\rho_{cc'}(\vec{r}) = \left\langle \Phi_{c'} \left| \sum_i \delta(\vec{r}-\vec{r}_i) \right| \Phi_c \right\rangle$$

Selectivity:

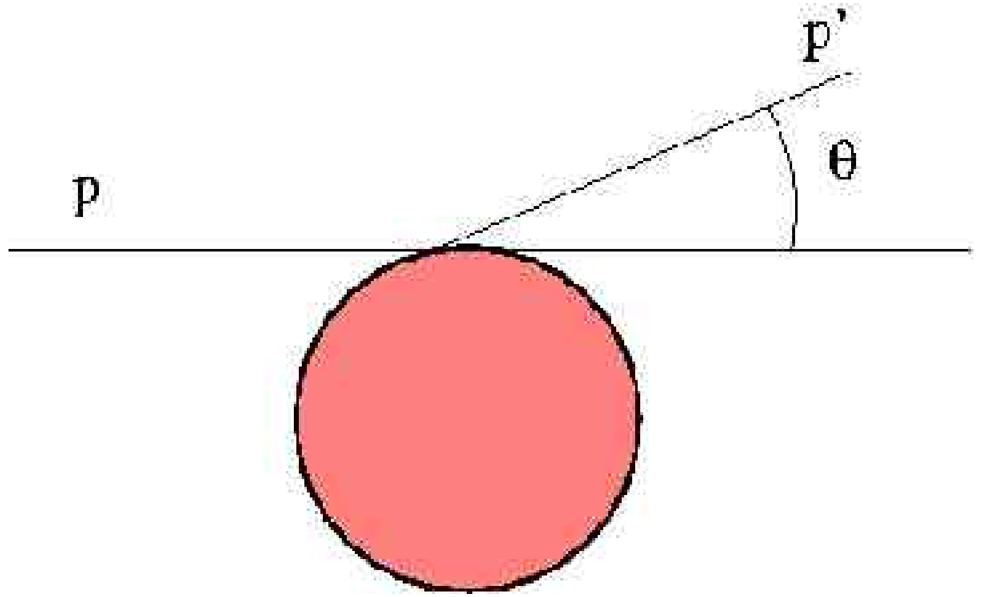

$$\vec{l} \approx \vec{k} R, \qquad \vec{l}' \approx \vec{k}' R, \qquad \Delta \vec{l} \approx \vec{q} R$$

$$\frac{d\sigma}{d\Omega} \propto \left| j_\lambda(qR) \right|^2 \qquad\qquad \lambda = \left| \vec{l} - \vec{l}' \right|$$

SI: J & parity

Special cases: Coulex, (e,e')

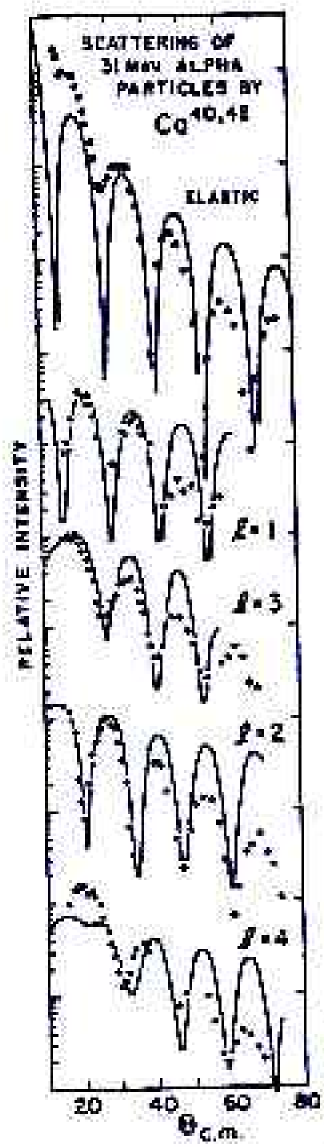

FIG. 4.1. Comparison of the Blair theory with experimental data for the elastic and inelastic scattering of 31-MeV α-particles by $^{40,42}Ca$. The elastic and $\ell = 1$ data for ^{40}Ca, all others are for ^{42}Ca. [From Austern (70).]

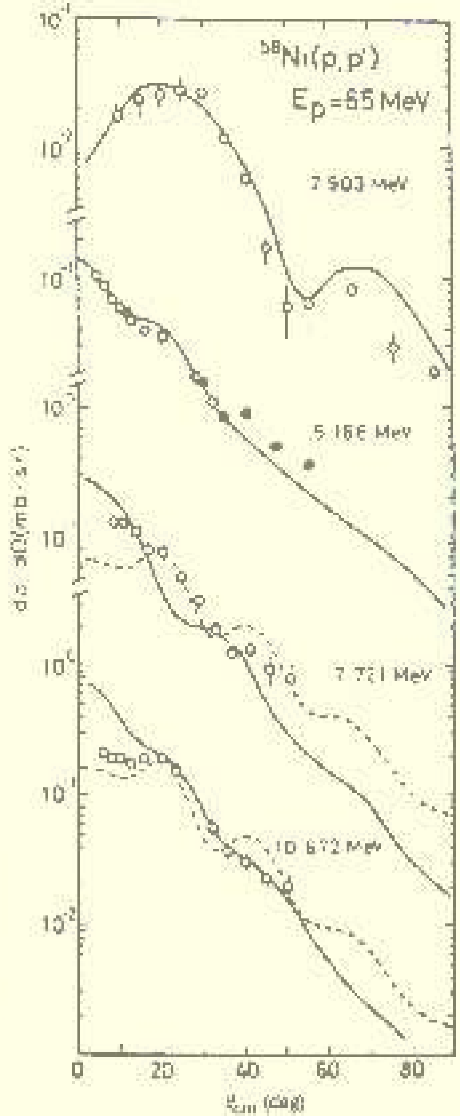

FIG. 6.8. Differential cross sections for the peaks corresponding to the 2.903$^-$, 5.166$^-$, 7.721$^-$, and 10.672 MeV states in ^{58}Ni. The solid curves are the microscopic DWA predictions calculated with the M3Y interaction [Bertsch, Borysowicz, McManus, and Love (77).] The results of the collective $L = 3$ DWA calculations are shown for comparison by the dashed curves. [From Fujiwara, Fujita, et al. (83).]

@ higher energy transfer:
excitation of giant resonances

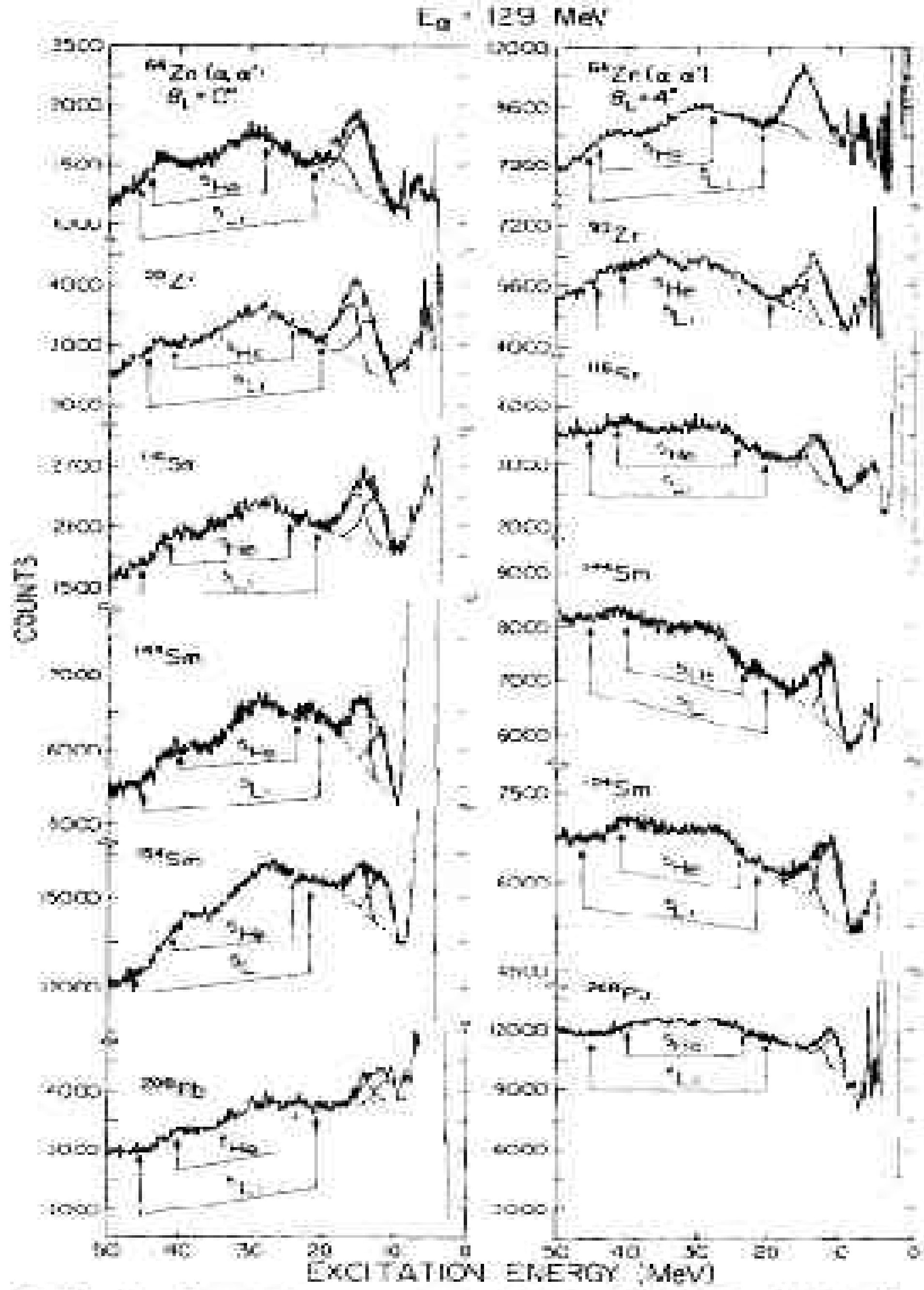

FIG. 1. Inelastic α spectra obtained at 0° and 4°. The GQR and GMR peaks and the background on which they reside are indicated. The regions where ^{5}He and ^{6}Li breakup would contribute are also indicated.

selectivity of probes

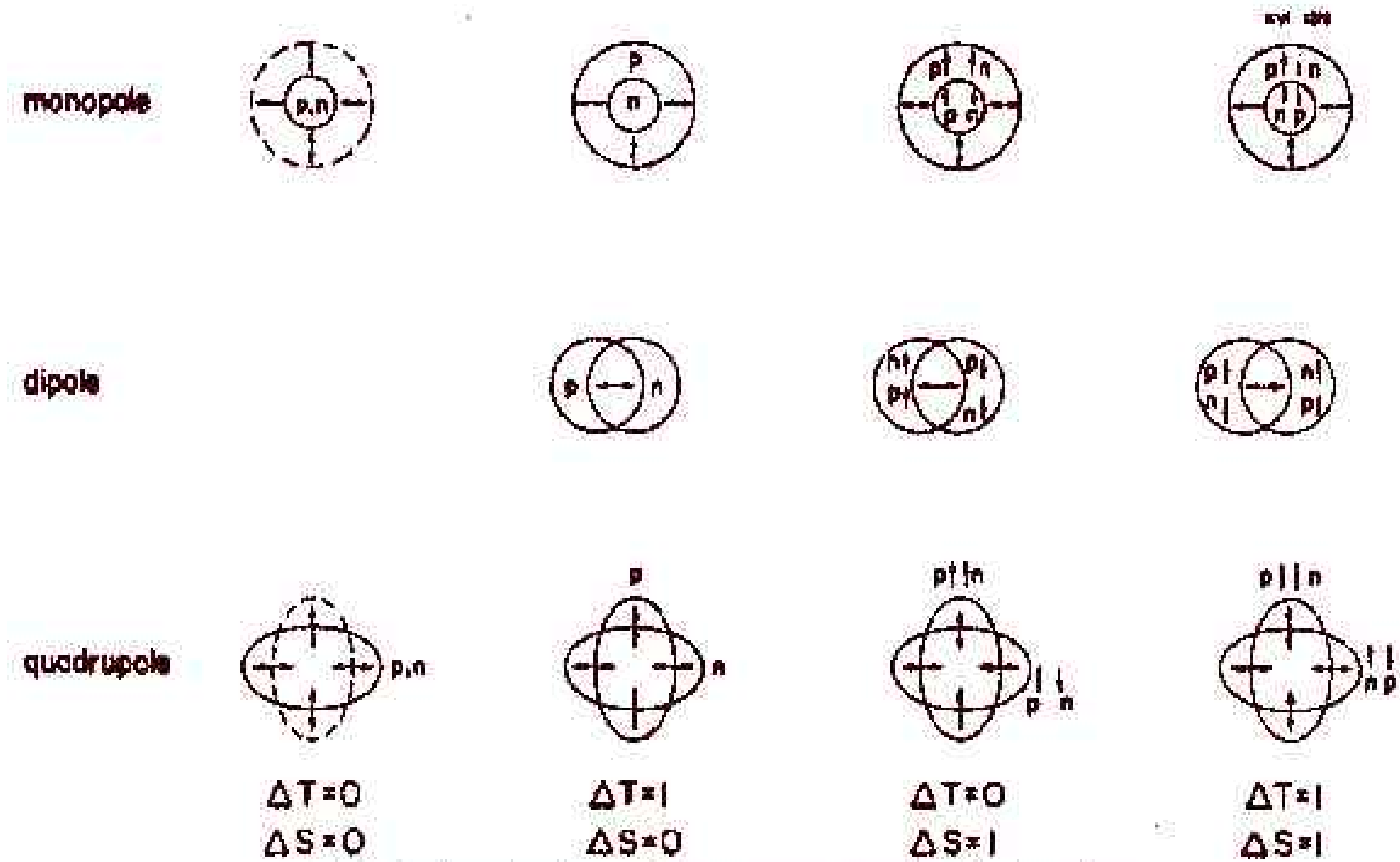

FIG 2. Qualitative picture of giant resonance modes of the nucleus.

(α,α') (p,p') (^{3}He,t)

SI: *giant resonances structure, sum rules, exchange forces*

D. Transfert reactions. Stripping, Pick-up, etc

Stripping: (d,p)

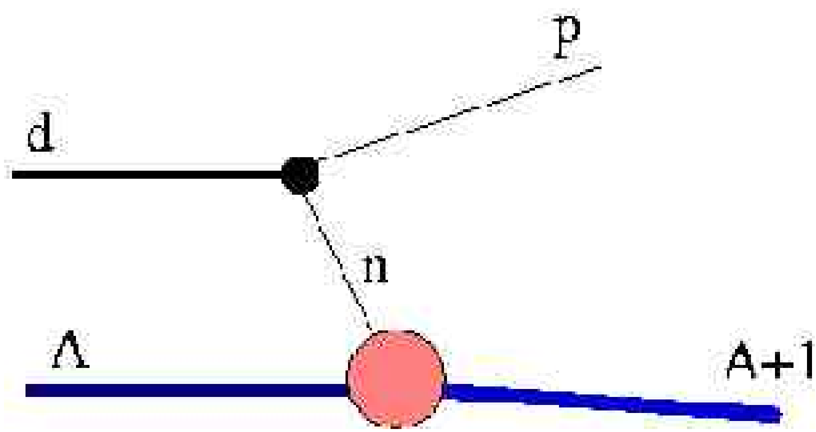

$$T \propto \Gamma_{d,pn}(\vec{q}) \frac{1}{\epsilon - \hbar^2 q^2 / 2 m_n} \Gamma_{B,An}(\vec{q})$$

- q should not be too large
- angular momentum selection rule

SI: Spectroscopic factors

$$\Phi_{A+1} = \sum_{\alpha} S_{\alpha}^{1/2} \varphi_{\alpha}(\vec{r}) \Phi_{A} \qquad (\alpha = nlj)$$

$$\frac{d\sigma}{d\Omega} = C D_0^2 S_{\alpha} \left| \int d^3(\vec{r}) \chi_d^*(\vec{r}) u_{\alpha}(\vec{r}) \chi_p(\vec{r}) \right|^2$$

$$S_{\alpha} = \left| \left\langle \varphi_{\alpha}(\vec{r}) \Phi_{A} \middle| \Phi_{A+1} \right\rangle \right|^2$$

$$\sum S_{\alpha} = 1 - N_{\alpha}$$

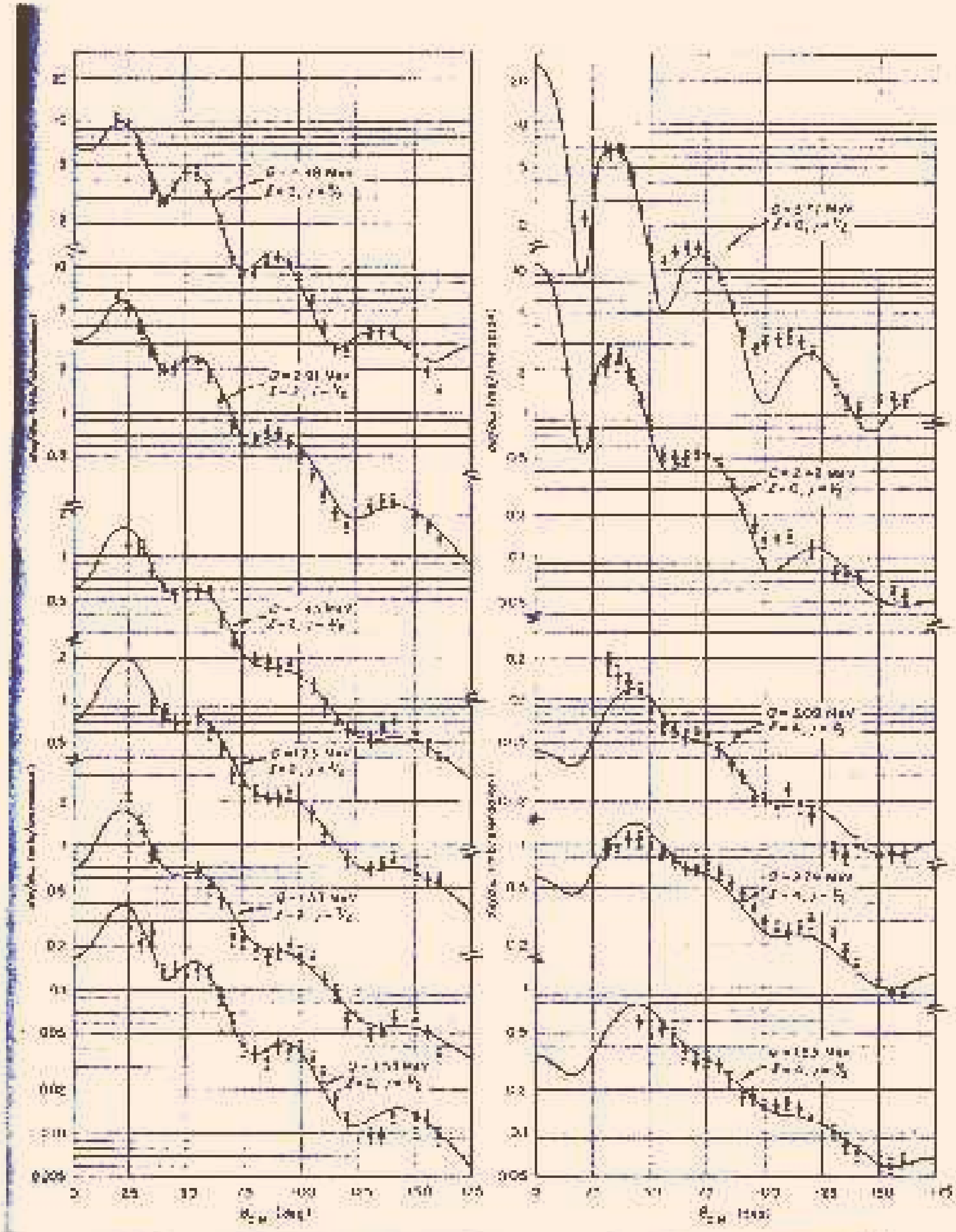

$^{90}Zr(d,p)$

E=12 MeV

Knock-out: (p,2p)

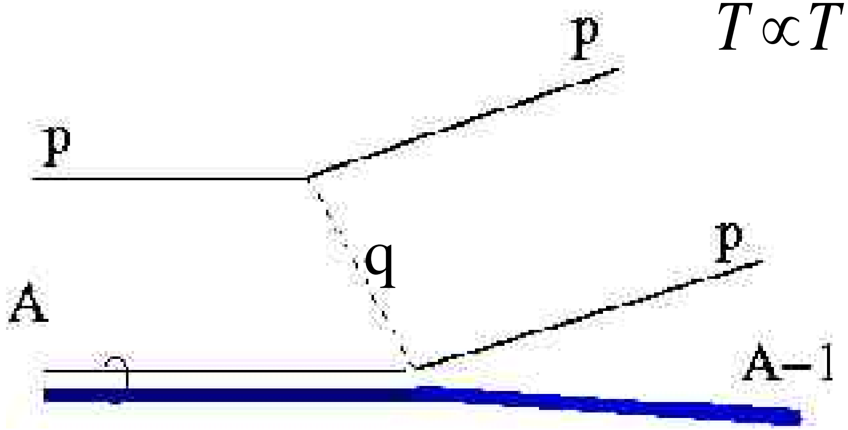

$$T \propto T_{pp}(\vec{q})\,\Gamma_{A,(A-1)p}(\vec{p}_R),\ \vec{p}_R = \vec{p}_2 - \vec{q},\ \vec{p}_1 = \vec{p}_i - \vec{q}$$

$$\frac{d^5\sigma}{dE_1\,d\Omega_1\,d\Omega_2} = C\,S_\alpha \left|\varphi_\alpha(\vec{p}_R)\right|^2 \frac{d\sigma_{pp}}{d\Omega}(\vec{q})$$

SI: momentum distribution of sp w.f. + spectroscopic factors

NB: (e, e' p) is simpler

4. Incoherent high-energy reactions

A. Introduction

- above ~ 250 MeV: dominance of NN collisions
- elastic scattering is limited to extreme forward angles, even though the cross section remains important (see later)
- angular momentum -> impact parameter as the relevant parameter
- coherent inelastic scattering is limited to very peripheral collisions (and to very forward angles)
- opening of huge number of channels: many ejected particles

  -> fragmentation

B. Glauber models

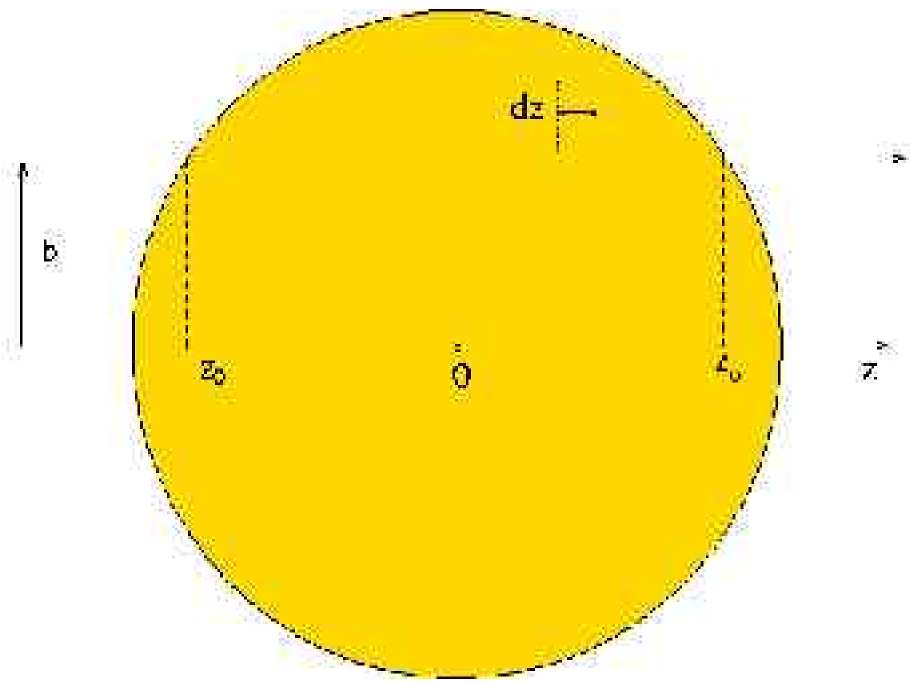

$$P_{surv}(z) = \exp(-\sigma_{NN}^{tot}\rho(z+z_0))$$

$$\sigma_R = \int_0^R 2\pi b\,db \int_{-z_0}^{z_0} P_{surv}(z)\rho\sigma_{NN}^{tot}dz = \pi R^2\left[1 - \frac{2}{X^2}(1-e^{-X}) + \frac{2}{X}e^{-X}\right]$$

$$X = 2\rho\sigma_{NN}^{tot}R \approx R \quad \rightarrow \quad \sigma_R \approx 0.8 - 0.9\pi R^2 \approx \sigma_E$$

A simplified quantum model: Glauber formalism + eikonal

basic assumptions: - small momentum transfer at each interaction
- scattering introduces a phase shift only: $e^{i\vec{k}.\vec{r}} \rightarrow e^{i\phi(\vec{r})}$
- frozen nucleus approximation (no Fermi motion)

$$f_{fi}(\vec{q}) = \frac{ik}{2\pi} \int d^2\vec{b}\, e^{i\vec{q}.\vec{b}} \left\langle \Phi_f \left| 1 - \prod_{j=1}^{A} \left(1 - \frac{1}{2i\pi k} \int d^2\vec{q}\,' e^{i\vec{q}\,'.(\vec{b}-\vec{s}_j)} f_j(\vec{q}\,') \right) \right| \Phi_i \right\rangle$$

f_j is the individual amplitude, $\mathbf{s}_j$ is the tranverse position of nucleon j

Expanding the product →multiple scattering expansion $f_{ij}(\vec{q}) = f_{ij}^{(1)}(\vec{q}) + f_{ij}^{(1)}(\vec{q}) + \ldots$

$$f_{ij}^{(1)}(\vec{q}) = f(\vec{q})\rho_{ij}(\vec{q}), \quad \rho_{ij}(\vec{q}) = \int d^2\vec{s}\, e^{i\vec{q}.\vec{s}} \left\langle \Phi_f \left| \sum_k \delta(\vec{s}-\vec{s}_k) \right| \Phi_f \right\rangle$$

SI: *transition prob.*

$$f_{ij}^{(2)}(\vec{q}) = \int d^2\vec{q}\,' f(\vec{q}) f(\vec{q}-\vec{q}\,') \rho_{ij}^{(2)}(\vec{q}), \quad \rho_{ij}^{(2)}(\vec{q}) = \int d^2\vec{s}\, d^2\vec{s}\,' e^{i\vec{q}.\vec{s}} e^{i(\vec{q}-\vec{q}\,').\vec{s}\,'} \left\langle \Phi_f \left| \sum_{k\neq l} \delta(\vec{s}-\vec{s}_k)\delta(\vec{s}-\vec{s}_l) \right| \Phi_f \right\rangle$$

SI: *correlations*

C. Models for collision regime

For many particle emission and deep inelastic collisions,
Glauber and quantum multiple scattering theories (KMT,..)
are unpracticable
Except for very peripheral and slightly inelastic collisions,
no evidence for quantum effects

Quasi-classical tools have been devised, where quantum effects
is restricted to small binary collision regions and translated in using
cross sections.

INC, QMD, BUU, LV,...

They are based on simulations and/or transport equations

INC

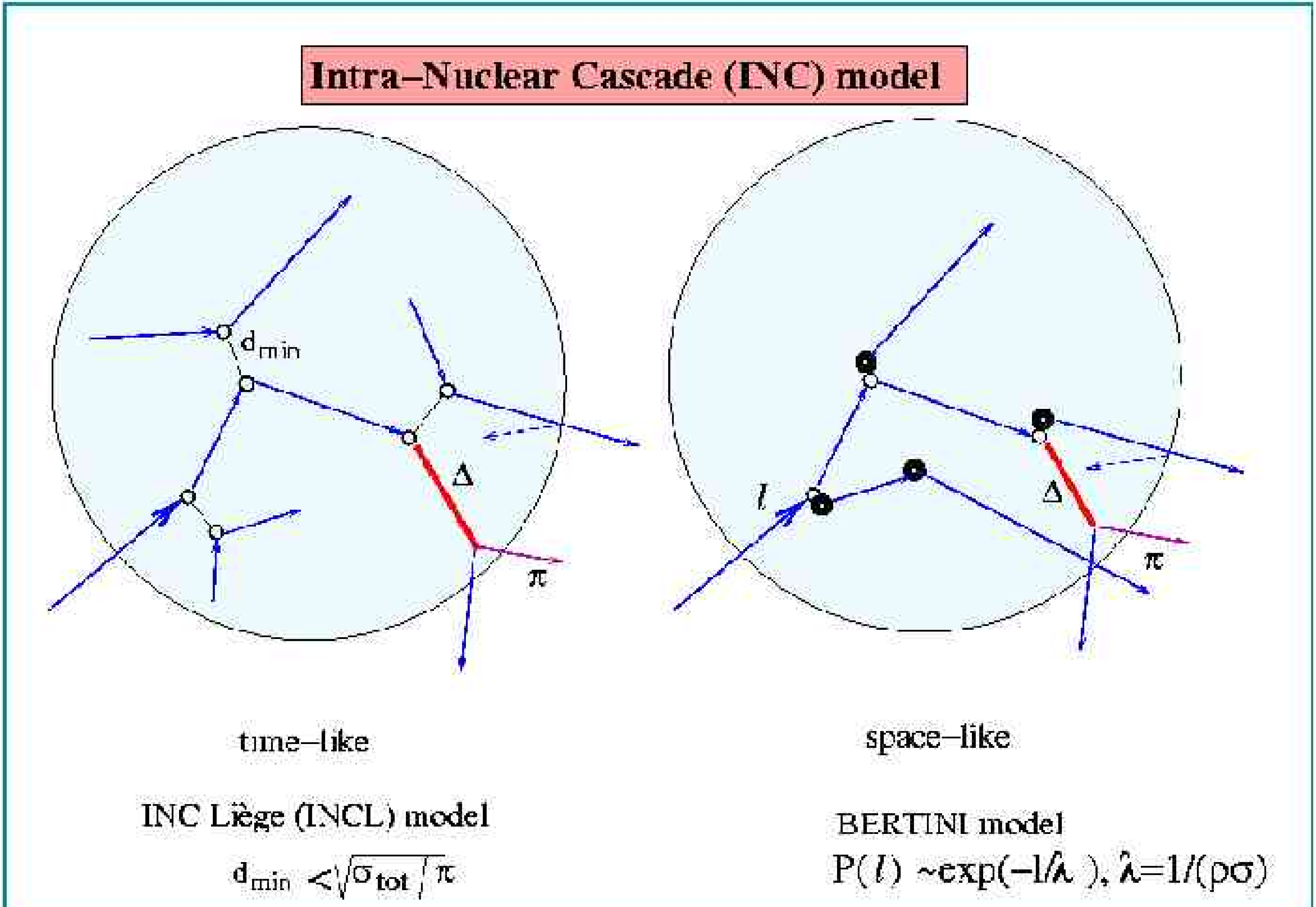

Intra–Nuclear Cascade (INC) model
d min
Δ
π
l
Δ
π
time–like
space–like
INC Liège (INCL) model
$d_{min} < \sqrt{\sigma_{tot} / \pi}$
BERTINI model
$P(l) \sim \exp(-l/\lambda), \lambda = 1/(\rho\sigma)$

brief description of INCL:

- ordered & separated NN collisions
- elastic or inelastic
- subject to Pauli blocking†
- potential well†
- transmission, reflection, (refraction)†
- stochasticity†
- relativistic kinematics
- isospin degree of freedom
- accomodates p, n, d, t, He3 & He4 as projectiles

- must be supplemented by an evaporation model
- stopping time is determined self-consistently

"*parameter-free*" SI: *geometry & momentum distribution*

D. Spallation and fragmentation collisions

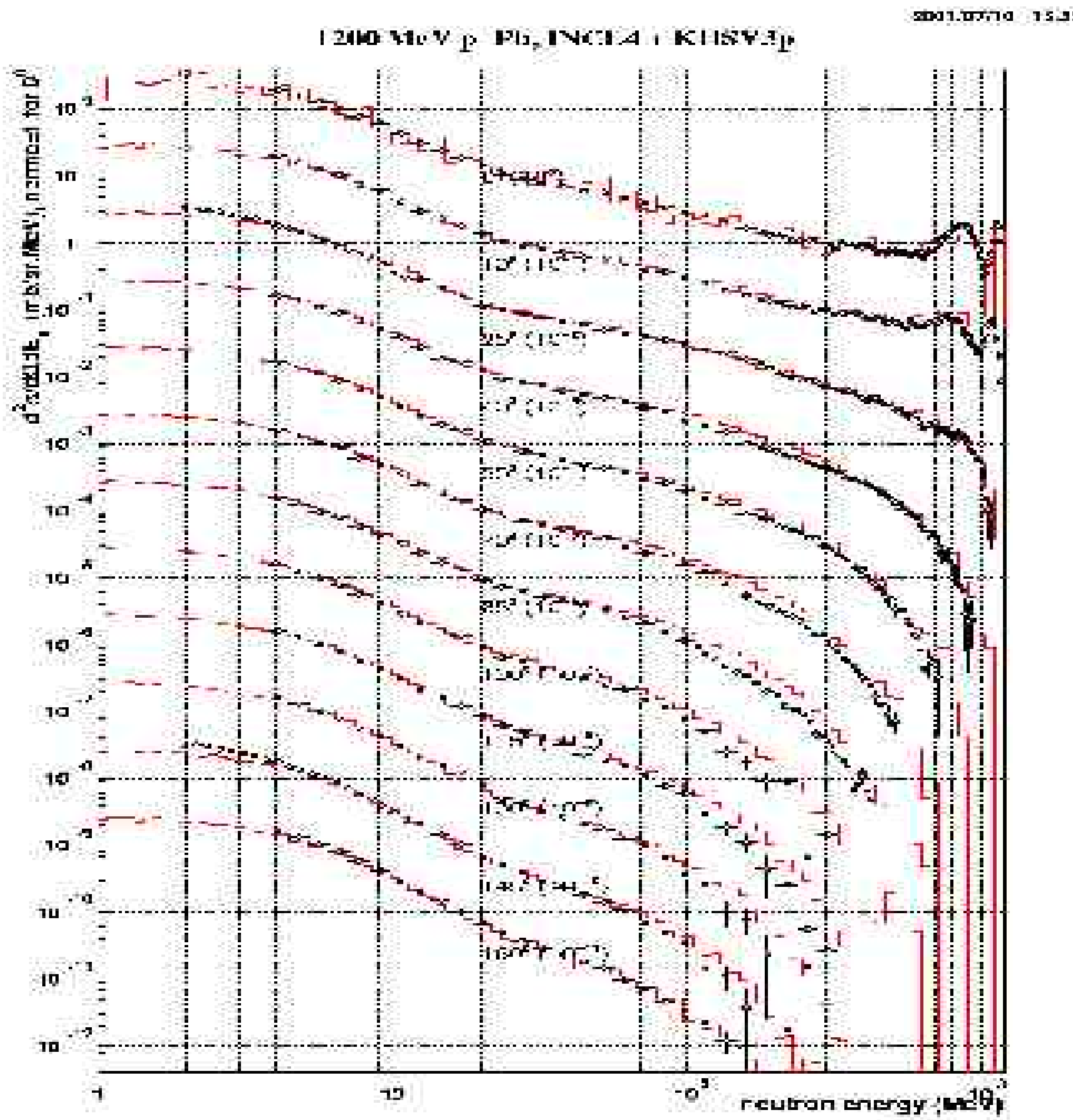

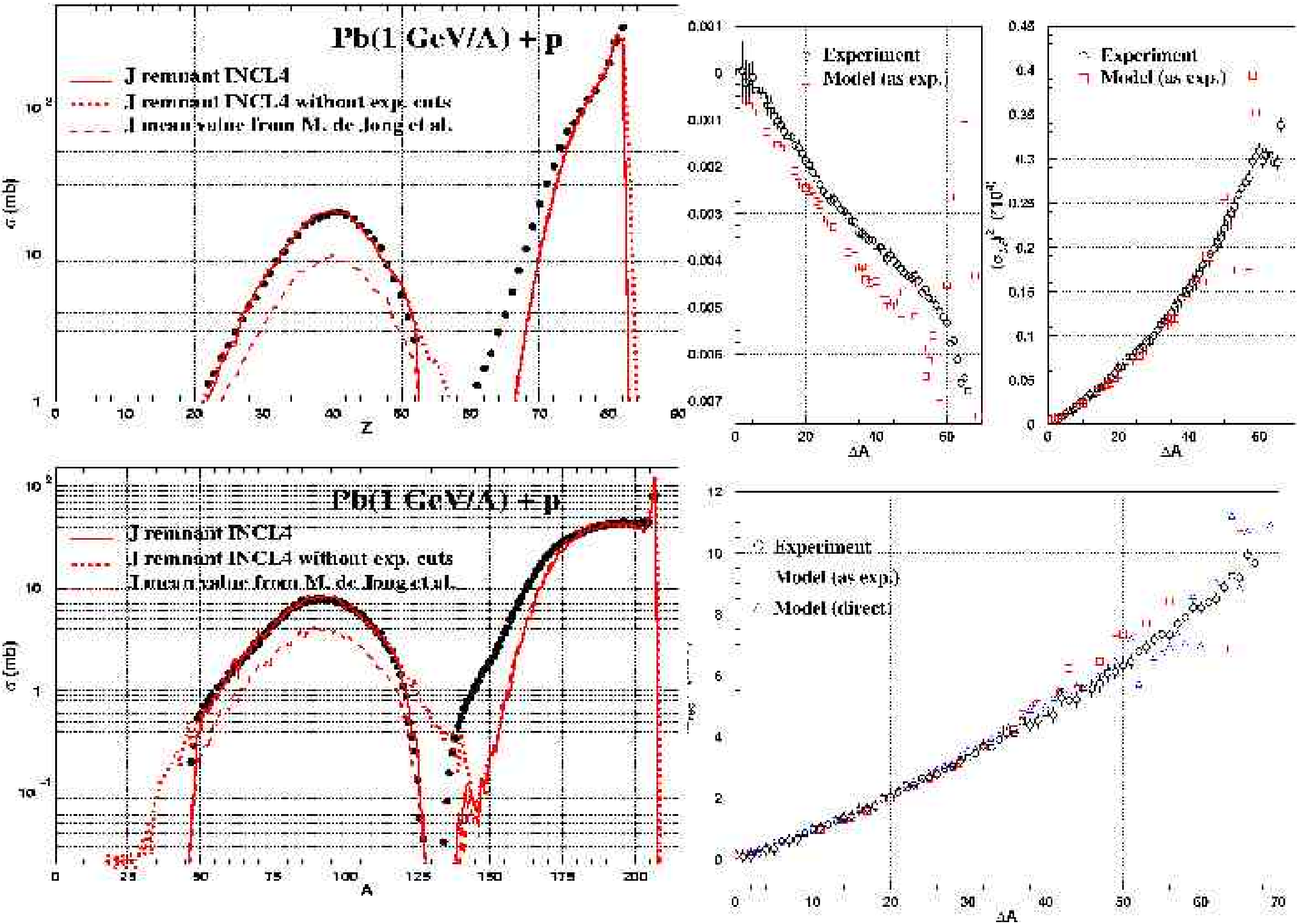
Pb(1 GeV/A) + p
J remnant INCL4
J remnant INCL4 without exp. cuts
J mean value from M. de Jong et al.
σ (mb)
Z
Experiment
Model (as exp.)
ΔA
Pb(1 GeV/A) + p
J remnant INCL4
J remnant INCL4 without exp. cuts
J mean value from M. de Jong et al.
σ (mb)
A
Experiment
Model (as exp.)
Model (direct)
ΔA

5. Reactions involving statistical coherent and incoherent features

A. Similarity between resonant reactions in the "overlapping regime" and the ultimate stage of spallation/fragmentation collisions

In the former, the reaction can be described by the formation of CN followed by an "independent" decay governed by average decay widths (Hauser-Feshbach)

Note that the formation of CN involves average over many different states, i.e. many degrees of freedom ⇒ equilibrated system

At the end of "hard collision" stage of spallation reactions, the system is also expected to be in equilibrium

HF for many exit channels

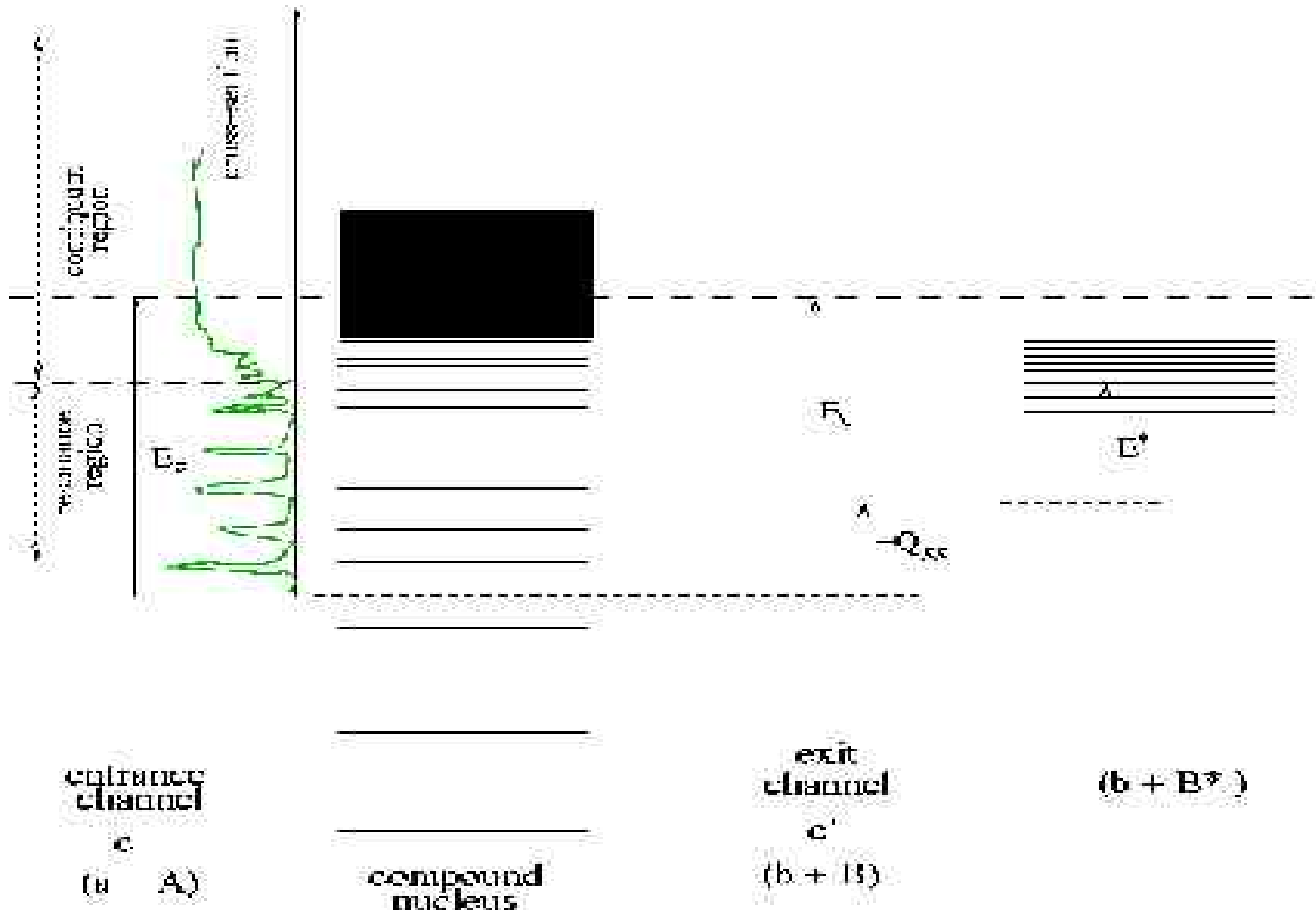

$$d\sigma_{HF}(E^*_{c'}) = \pi \lambda_c^2 \frac{T_c T_{c'} \omega_{c'}(E^*_{c'})\, dE^*_{c'}}{\sum_{c''} \int_0^{E+Q} T_{c''} \omega_{c'}(E^*_{c''})\, dE^*_{c''}}$$

NB: HF is limited to low energy, but includes angular momentum

B. Evaporation-fission and other de-excitation models

The Weisskopf-Ewing evaporation model

Let us assume A*→B*+b in a volume V; $E^*=E_B^*+S+\epsilon$

Probability of emission per unit time:

$$d\Gamma_b = \frac{2\pi}{\hbar}\left|\langle A|T|B\,b\rangle\right|^2 \omega(E_B^*)\frac{V k^2 dk}{(2\pi)^3} \qquad \sigma^{CN}(bB^* \to A^*) = \frac{2\pi}{\hbar}\frac{\left|\langle bB|T|A\rangle\right|^2 \omega(E_A^*)}{\hbar k/mV}$$

$$d\Gamma_b = \sigma^{CN}(bB^* \to A^*)\frac{2m}{(2\pi)^3\hbar^2}\frac{\omega(E_B^*)}{\omega(E_A^*)}\epsilon\, d\epsilon$$

can be used for calculating X-sections $\quad d\sigma(\varepsilon) = \sigma_c^{CN}\dfrac{d\Gamma_b}{\sum\limits_b \int\limits_0^{E-S} d\Gamma_b}$

For $\omega(E^*) = p\exp(2\sqrt{aE^*})$ and $E^*=aT^2$

$$\Gamma_b = \sigma^{CN}(bB^* \to A^*)\frac{2mT^2}{(2\pi)^3\hbar^2}e^{-S/T}$$

$$d\Gamma_b \propto e^{-\epsilon/T}\epsilon\, d\epsilon$$

fission

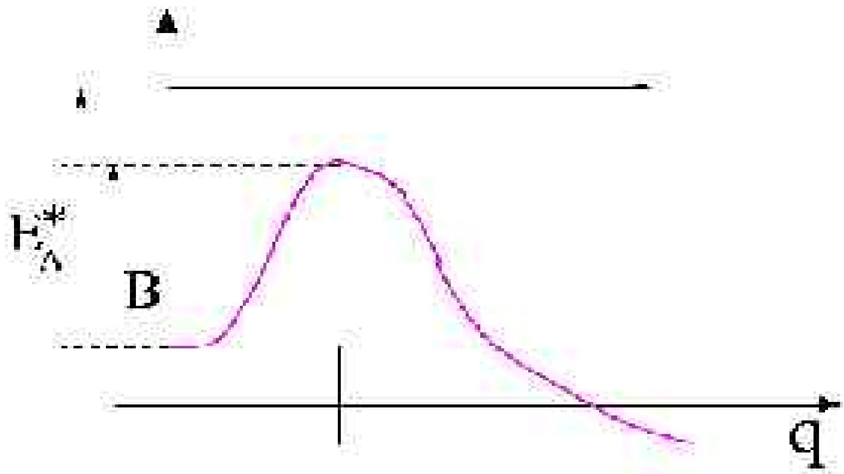

everything is determined by phase space at the barrier

$$E_A^* = E_B^* + B + p^2/2m$$

$$\frac{d\Gamma_f}{\hbar} = \frac{\omega_B(E_B^*)\, dE_B^*\, (dp\, dq/2\pi\hbar)/dt}{\omega_A(E_A^*)\, dE_A^*}$$ and $$dq/dt = p/M\,,\ Mpdp = d\epsilon$$

$$d\Gamma_f = \frac{1}{2\pi} \frac{\omega_B(E_B^*)}{\omega_A(E_A^*)} d\epsilon \quad \Rightarrow \quad \Gamma_f = \frac{T}{2\pi} e^{-B/T}$$

must be supplemented by a fission partition model

SI: *level density & barriers*

Other “after-burning” models

1. evaporation: simulation of successive separated emissions

time scales $\tau_b = \hbar / \Gamma_b \gg t_{emiss}(b)$

2. for increasing temperature τ_n may become smaller than t_{emiss} (fission

neutrons may be emitted from the system on its way to fission=

fission delayed or friction in fissioning motion

3. above some “temperature” ►► copious simultaneous emission

✸ multifragmentation

- usual models include any partition of the system
- final states = partitions of an equilibrated system (SMM, ...)

SI: *thermodynamics of nuclear matter / possible phase transition*

C. Pre-equilibrium reactions

For resonant reactions in the "continuum", if energy increases (above ~ 20 MeV), the spectra are no longer thermal & emission no longer isotropic

Idea = addition of fast +/- coherent emission and slow evaporation

Many special tools:

- HF+DR
- Harp-Miller-Berne sp model
- exciton model
- hybrid model
- GDH model
- FKK theory
- ...

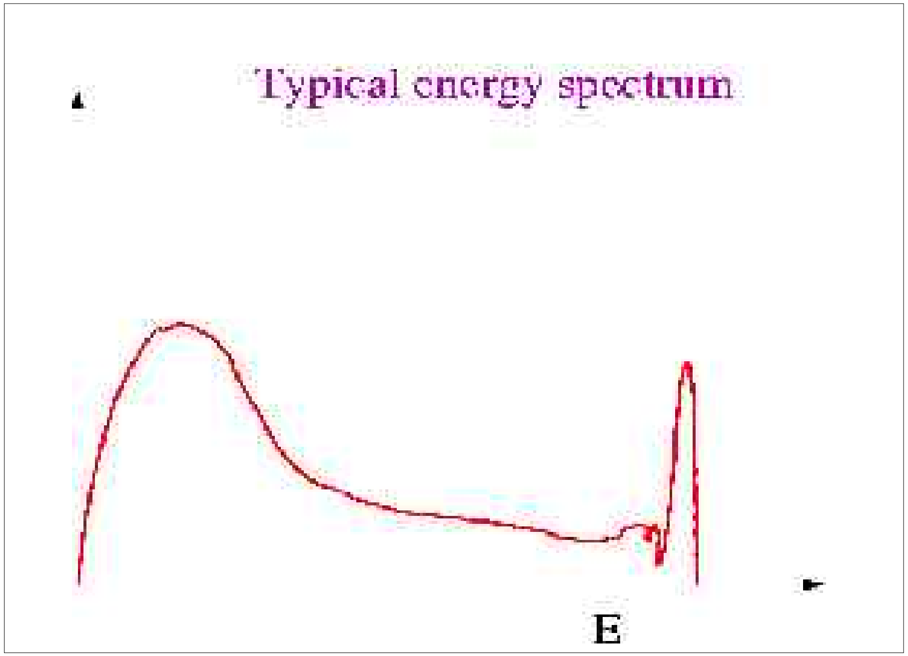

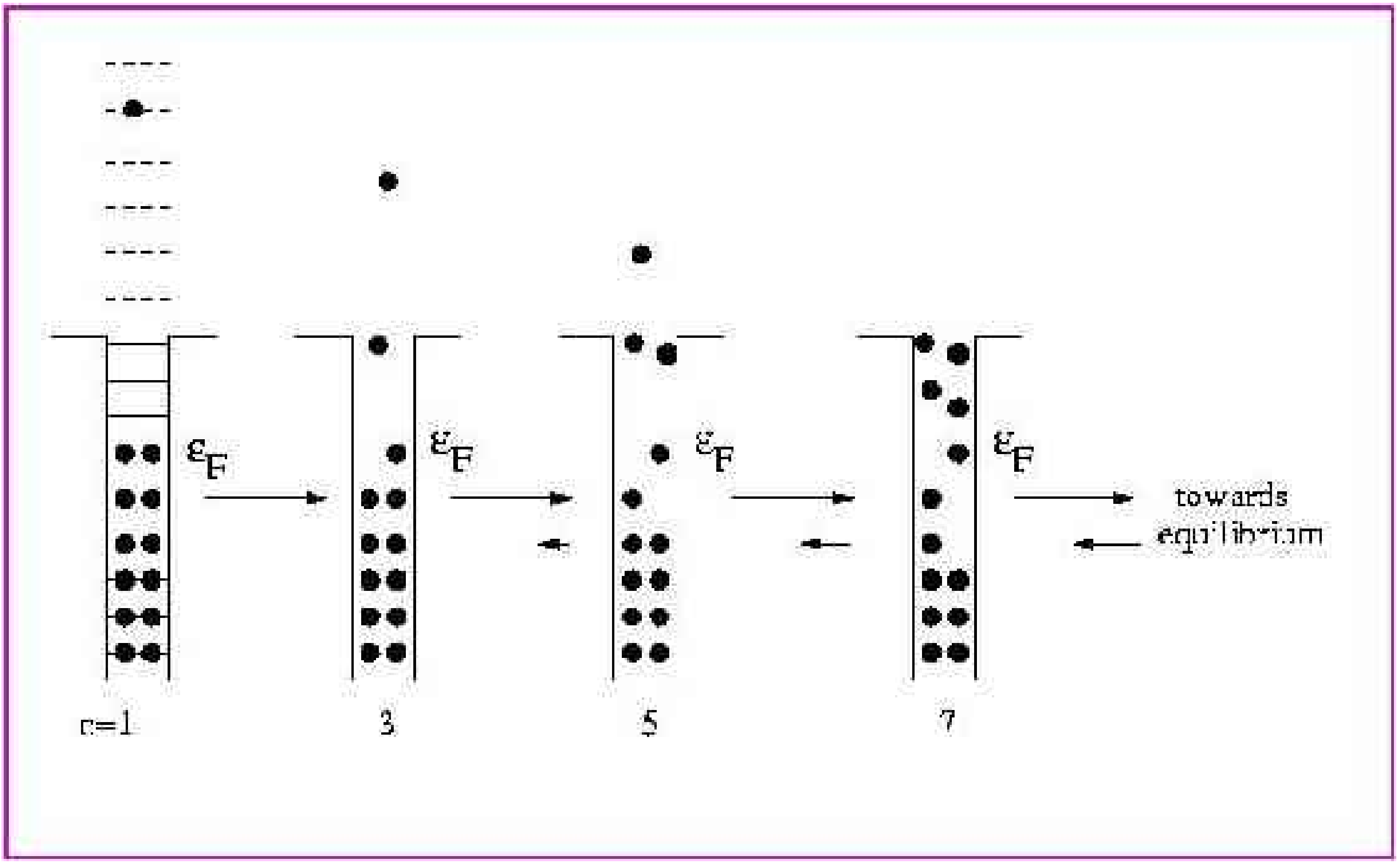

ε_F
ε_F
ε_F
ε_F
towards
equilibrium
n=1
3
5
7

1. *Harp-Miller-Berne approach*

-initial state: n_i=1 for $k_i < k_F$ and $k_i = k_c$, k_i =0 otherwise

-evolution:

$$\frac{dn_i}{dt} = \sum_j \sum_k \sum_l \omega_{ijkl} \left\{ n_k n_l (1-n_i)(1-n_j) - n_i n_j (1-n_k)(1-n_l) \right\} - \lambda_{esc} n_i$$

$$\omega \approx \rho \sigma_{NN} \langle v \rangle$$

-prediction of spectra

$$\frac{dP(\epsilon)}{d\epsilon} = \int_0^T dt \sum_i \lambda n_i(t) \delta(\epsilon - \epsilon_i)$$

- abandoned, due to the numerical task

2. *The exciton model (J. Griffin)*

-whole distribution →exciton states 1p, 2p-1h, 3p-2h,...(n=1,3,5,7...)

-density of (n=p+h) exciton states of given energy E (Ericson)

$$\rho_n(E)=\frac{g^n E^{n-1}}{p!h!(n-1)!}$$

-probability of emission from a n-exciton state per unit time

$$P_n(\epsilon)d\epsilon=\frac{m\epsilon}{\pi^2\hbar^3}\frac{\rho_{n-1}(U)}{\rho_n(E)}d\epsilon \qquad U=E-S-\epsilon$$

-spectrum

$$P(\epsilon)d\epsilon=\sum_{n=n_0}^{\bar{n}}\tau_n P_n(\epsilon)d\epsilon=\frac{m\epsilon}{\pi^2\hbar^3}\sum_{n=n_0}^{\bar{n}}\frac{\rho_{n-1}(U)}{\rho_n(E)}\tau_n d\epsilon$$

-exciton hybrid model (*M. Blann*)

$$\frac{d\sigma}{d\epsilon}=\sigma_R\sum_{n=n_0}^{\bar{n}}\left[\frac{m\epsilon}{\pi^2\hbar^3}\frac{\rho_{n-1}(U)}{\rho_n(E)}d\epsilon\right]\left[\frac{P_n(E)}{P_n(E)+\lambda_+^{n+2}(E)}\right]D_n=\sigma_R\sum_{n=n_0}^{\bar{n}}P^{(n)}(\epsilon)d\epsilon$$

$$D_n=\prod_{n'=n_0}^{n-2}\left\{1-\int P^{(n')}(\epsilon)d\epsilon\right\},\quad D_{n_0}=1$$

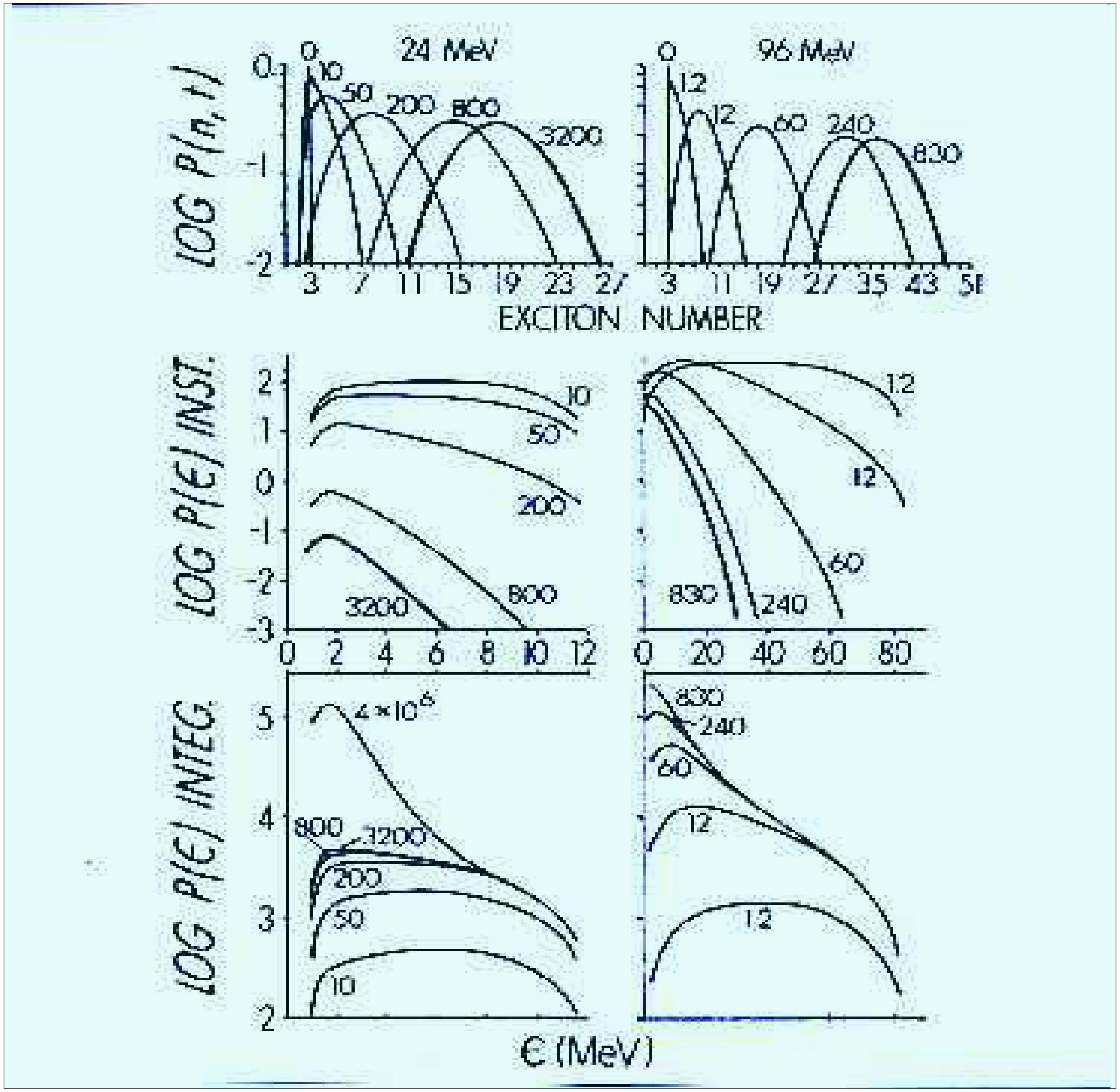

24 MeV
96 MeV
LOG P(n, t)
EXCITON NUMBER
LOG P(ε) INST.
LOG P(ε) INTEG.
ε (MeV)

M. Blann

$$\lambda_{+}^{n+2}(\epsilon)=\frac{2\pi}{\hbar}\overline{|M|^2}\rho(E^*) \quad \text{or} \quad \lambda_{+}^{n+2}(\epsilon)=\frac{\lambda}{v}=1/\rho\sigma_{NN}v=2\frac{W}{\hbar}$$

OMP → W

$$\overline{|M|^2}=KA^{-3}E^{-1}$$

SI: density of exciton states, mfp

further developments:

- cross-sections (GDH): $\frac{d\sigma}{d\varepsilon} = \int 2\pi b\, db\, P_b(\varepsilon)$

- angular distributions:

$$\frac{d\sigma}{d\varepsilon\, d\Omega} = \sigma_R \sum_{n+n_0}^{\bar{n}} P^{(n)}(\varepsilon) \sum_L \frac{2L+1}{4\pi} f_L(n) P_L(\cos\theta)$$

with f_L= parameters (Kalbach)

- emission of clusters, through phenomenological probabilities attached to every n-exciton state

3. *The Feshbach-Kerman-Koonin (FKK) theory*

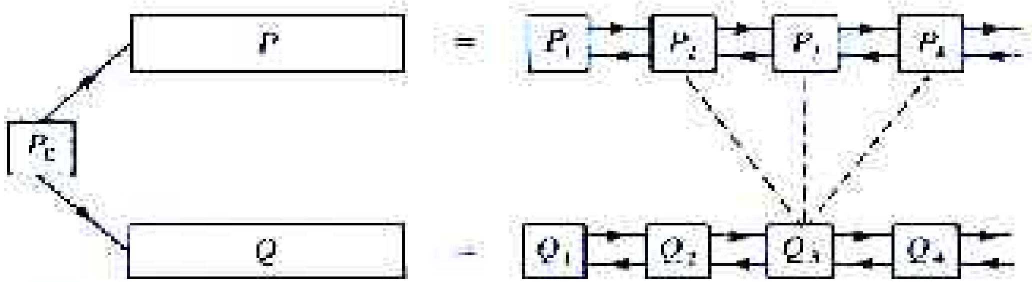

Multistep description of a nuclear reaction (Feshbach *et al.* 1980).

P-chain=MSD=at least one particle is unbound

Q-chain=MSC=all particles are bound

FKK:

-no communication between P and Q-chains

-chaining only between n and n$\pm$1 states

-never-come-back hypothesis (n -> n+1)

MSC:

$$\sigma_{MSC} = \pi \lambda_c^2 \frac{2\pi \Gamma_1}{D_1} \sum_{n=1}^{r} \left(\frac{\prod_{k=1}^{n-1} \Gamma_k^{\downarrow}}{\Gamma_k} \right) \frac{\Gamma_n^{\uparrow}}{\Gamma_n}$$

$$\Gamma_n^{\uparrow} = \frac{2\pi}{\hbar} \overline{\left| \langle n | V | n+1 \rangle \right|^2} \rho_n(U) \rho(\epsilon) \qquad \Gamma_n^{\downarrow} = \frac{2\pi}{\hbar} \overline{\left| \langle n | V | n+1 \rangle \right|^2} \rho_{n+1}(E)$$

$$\langle n | V | n+1 \rangle \approx V_0 \int u_1(r) u_2(r) u_3(r) \begin{Bmatrix} u_{scatt}(r,\epsilon) \\ u_4(r) \end{Bmatrix} \frac{dr}{r^2}$$

MSD: $\frac{d^2\sigma_{MSD}}{d\Omega\, dU} = \frac{d^2\sigma_1}{d\Omega\, dU} + \frac{d^2\sigma_M}{d\Omega\, dU} \qquad \frac{d^2\sigma_1}{d\Omega\, dU} = \rho_r(U) \left\langle \frac{d\sigma}{d\Omega} \right\rangle$

$$\frac{d^2\sigma_M}{d\Omega_N\, dU_N} = \sum_N \int \frac{d^3 k_{N-1}}{(2\pi)^3} \cdots \int \frac{d^3 k_2}{(2\pi)^3} \frac{d^2 W_{N,N-1}(\vec{k}_N, \vec{k}_{N-1})}{d\Omega_N\, dU_N} \frac{d^2 W_{N_1,N-2}(\vec{k}_{N-1}, \vec{k}_{N-2})}{d\Omega_{N-1}\, dU_{N-1}} \cdots \frac{d^2 W_{2,1}(\vec{k}_2, \vec{k}_1)}{d\Omega_2\, dU_2} \frac{d^2\sigma_1}{d\Omega_1\, dU_1}$$

$$\frac{d^2 W_{N,N-1}(\vec{k}_N, \vec{k}_{N-1})}{d\Omega_N\, dU_N} = \frac{2\pi}{\hbar} \overline{\left| \int d^3\vec{r}\, \chi^{+}(\vec{k}_N) \chi^{-}(\vec{k}_{N-1}) \langle \psi_N | V | \psi_{N-1} \rangle \right|^2} \frac{m k_N}{(2\pi)^3 \hbar^2} \rho_r(U_N)$$

C. Comparison INC-preequilibrium models

- All have to be supplemented by evaporation
- Phase space is classical in INC, discrete in PE models
- Pauli blocking is more naturel in INC
- same common physics in all models: interaction in a Fermi gas mediated by binary collisions
- INC is a more consistent model (only the stopping is "by hand")
- more or less equivalent results below 200 MeV (where INC shouldn't work!!)

INC+evaporation= a theory from 40 MeV to 10 GeV?

6. Specific features linked to particular projectiles

A. Slightly bound nuclei

easy fragmentation

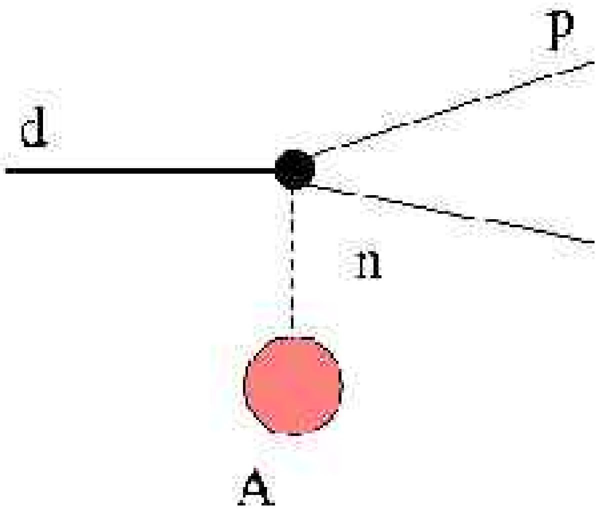

$$\vec{p}_1 = m\vec{v}_{inc} + \vec{p}_{internal}$$

$$\frac{d\sigma}{d^3\vec{p}_1} \propto f(\vec{p}_1)$$

SI: momentum distribution

surrogate reactions

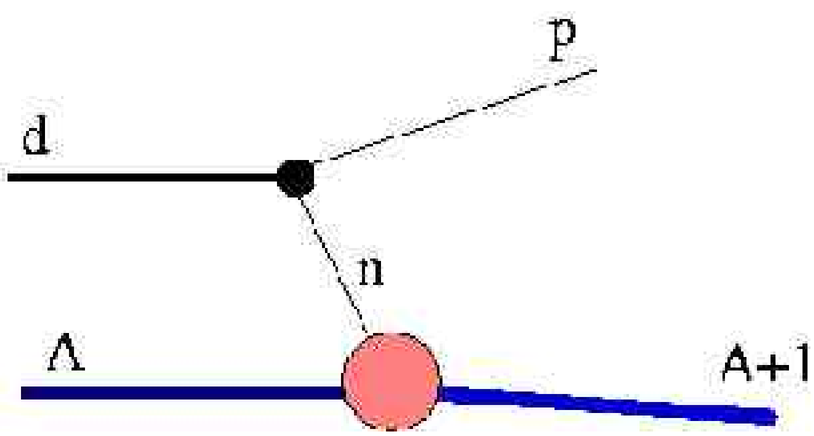

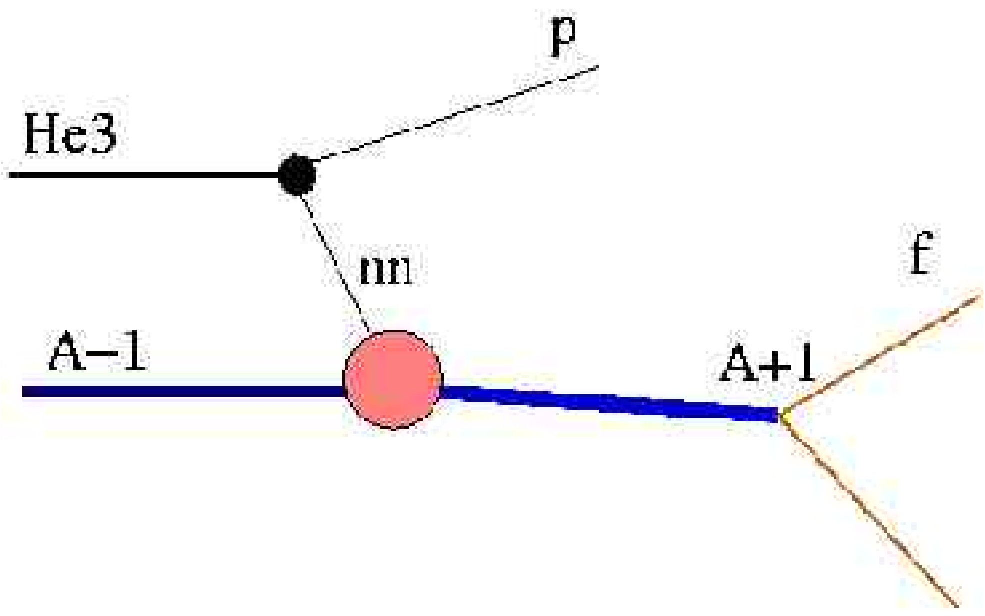

$$\frac{d\sigma}{d^3\vec{p}} = \frac{d\sigma}{d^3\vec{p}}\left({}^3He + (A-1) \rightarrow p + (A+1)^*\right)_{DWBA} \frac{\Gamma_f}{\Gamma_{tot}}$$

$$\sigma(n+A \rightarrow f) = \sigma_{NC}\left(n+A \rightarrow (A+1)^*\right) \frac{\Gamma_f}{\Gamma_{tot}}$$

B. Proton or neutron rich nuclei

study of isospin degree of freedom by inverse kinematics

IAS

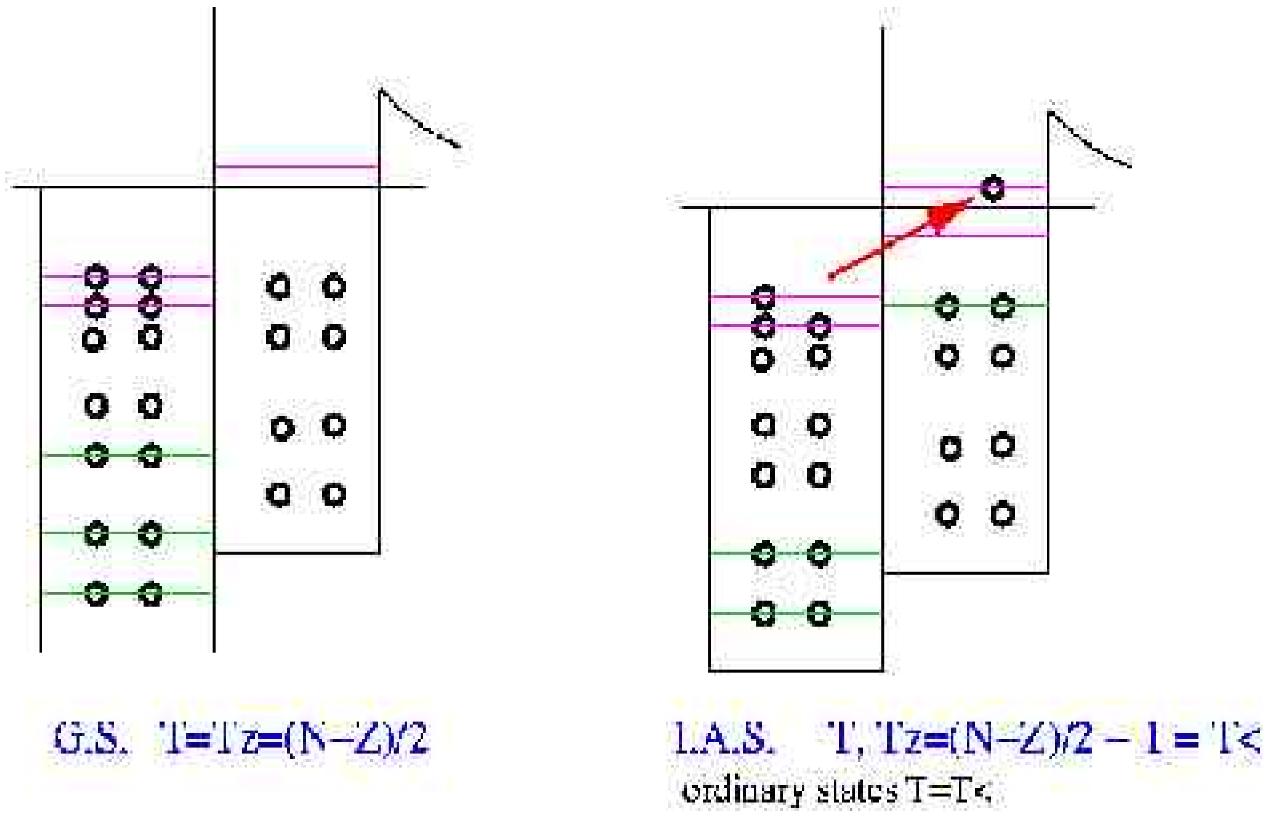

seen by resonant scattering ^{207}Pb(p,p) or by production ^{208}Pb(p,n)

ordinary spectroscopy by p(A,A*)p with recoil measurements

C. Photons

Real photons probe the nucleus with an elm field:

- very good for electric giant resonances ($\Delta T=1$)
- photodesintegration (γ,n)

Virtual photon (e,e) (e,e')

- charge density
- transition densities
- parton structure

D. Mesons, antiprotons, etc

pions

SI: surface densities, $\Delta S=1$, ΔT transitions, pair correlations

↓ elastic   ↓ inelastic   ↓ absorption

antiprotons

annihilation: ~2 GeV without p,ℓ transfer

good for study of hot nuclei

7. Summary & outlook

	elastic	*inelastic*	*profoundly inelastic*
nucleon-nucleus	elastic scattering *nuclear size & interaction potential*	inelastic scattering pick-up reactions resonant reactions *energy level location & quantum numbers* *giant resonances* fission	spallation *RIB*
nucleus-nucleus	*interaction potential* *strong absorption & diffractive scattering*	fusion reactions *new and SHE elements*	multifragmentation *phase transition* *EOS of nuclear matter*
meson-nucleus	*strong absorption limit*	*excitation of π d.o.f.*	*investigation of nuclear glue*
electron-nucleus	*nuclear size*		deep inelastic scattering *quark structure of nuclei*
neutrino-nucleus	*neutrino transparency*		*messages from the universe*

D. <u>The shell-model approach</u>

$$H = H_0 + V = \sum_i h_0(i) + V \qquad H_0 \varphi_i = E_i \varphi_i, \quad H_0 \chi_c(E) = E \chi_c(E)$$

$$\Psi_c^+ = \sum_i b_i(E) \varphi_i + \sum_{c'} a_c^{c'}(E) \chi_{c'}(E)$$

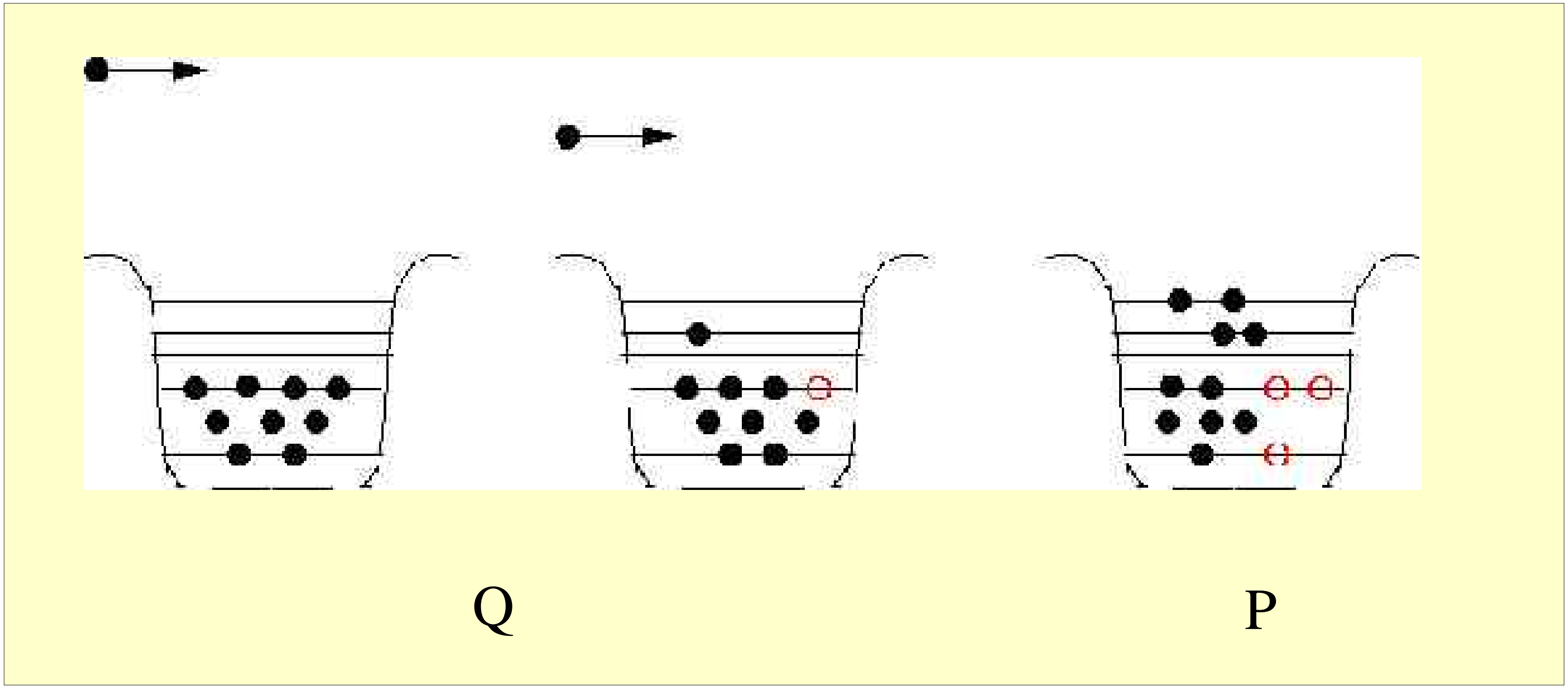

χ_E^c $\qquad$ $\chi_E^{c'}$ $\qquad$ φ_i

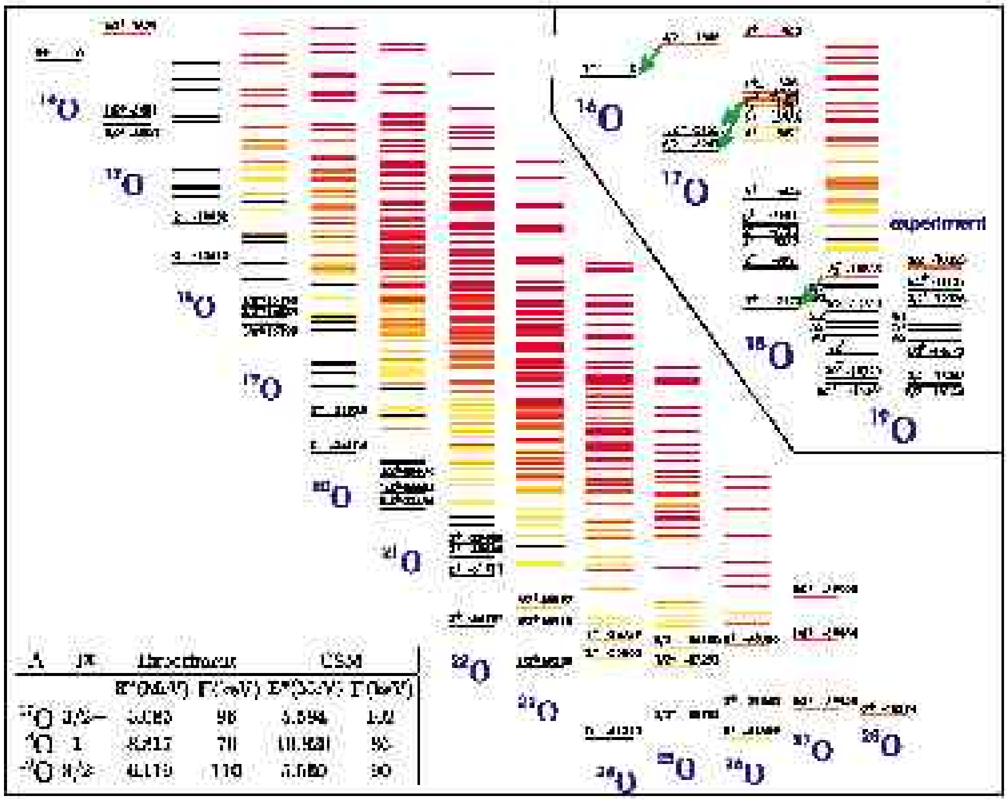

FIG. 2 (color online). CSM calculations for oxygen isotopes with the HBUSD interaction. States from yellow (long lifetime) to red (short lifetime) are resonance states. In black and white print these resonances are differentiated by shades of gray, from lighter to darker, respectively. States shown in black are stable in our model; they are either below decay thresholds or with decays forbidden due to the angular momentum restrictions in the selected valence space. The inset in the upper right shows a more detailed picture for the lightest ^{16}O to ^{19}O isotopes. Decays from all states that are experimentally measured are shown with arrows. A full comparison between available data and the calculation is given for ^{17}O. Energies are expressed in units of keV. A comparison of widths with available data is given in the table in the left lower corner. For both insets the interaction USD was used that works better for lighter isotopes.

A.Volya &V. Zelevinsky
PRL94(2005)052501

subsection we are primarily interested in the high-energy part of the (p,n) cross section.

Figure 15 shows the results for the reaction $^{89}Y(p,n)^{89}Zr$ with global parameter for the exciton model and GDH model. For comparison, we also show the HFDR result, taken from Fig. 12. Note that we took the value of $K = 400$ MeV^3 as default in the STAPRE code by arbitrary choice. This value is suggested by the work of the Milano group[46] and by our limited experience.[1] However, we have done calculations with parameters, $K = 405$ MeV^3 and $g = A/13$ MeV^{-1}, and appropriate transition rates as given by Kalbach.[47] The calculations show about 10% lower cross sections than those shown here for the exciton model. In this figure, we only show the default GDH results.

The calculated cross sections shown in Fig. 15 agree with the data to within 50%. However, the agreement can be significantly improved if one varies the parameter K in the exciton model (Fig. 16) and the mean-free path in the hybrid or GDH models (see Fig. 17). Similar agreement can also be achieved by adjusting the parameter g. Note also the successful analysis of the earlier (p,n) data by Birattari et al.[12] and Gadioli et al.[45] using the HF and a phenomenological preequilibrium model. These authors have analyzed data for many (p,n) reactions, but a good fit to the data always required an adjustable parameter.

We have not done an extensive analysis of the present data with many refinements of the exciton model. But we believe that the essential physics is included here. An open question, however, is the role of shell effects on the exciton state densities. This may be important since our target-projectile composite is a closed shell. This may be the reason why the global GDH model did not fit the data as well as we would have expected. Some progress in this regard has been reported by Sobel et al.[48]

Although our presentation in this section was limited to the (p,n) reaction, the arguments given for this reaction apply also to the (p,2n) and (p,pn) reactions. Our conclusion at this time is that present preequilibrium

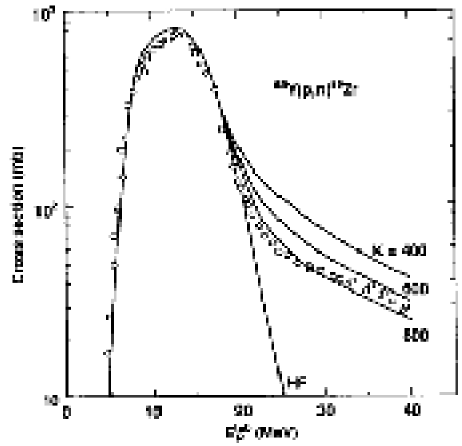

FIG. 16. The analysis of the $^{89}Y(p,n)^{89}Zr$ reaction. The results show the sensitivity of the cross sections with respect to the exciton model parameter K. Notice that a good fit to the data can be obtained.

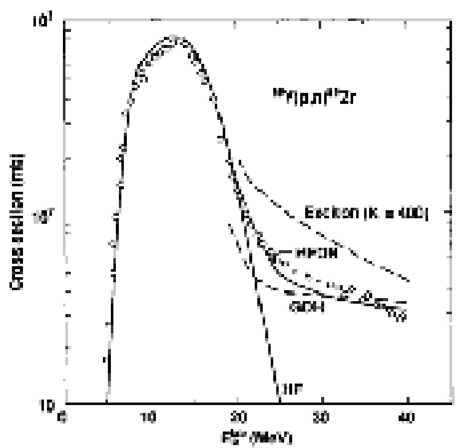

FIG. 15. The analysis of the $^{89}Y(p,n)^{89}Zr$ reaction. The Hauser-Feshbach (HF) plus one-step direct-reaction cross sections (HFDR) are compared with HF plus phenomenological preequilibrium model [exciton and geometry-dependent hybrid (GDH)] calculations with global parameters.

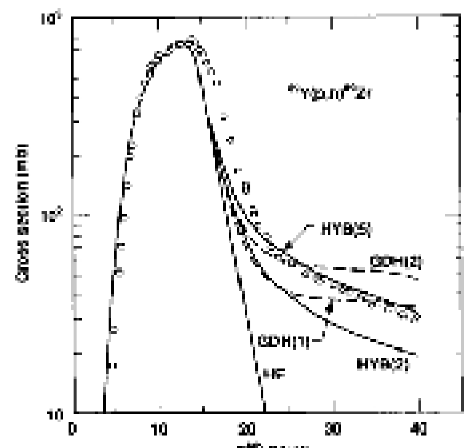

FIG. 17. The analysis of the $^{89}Y(p,n)^{89}Zr$ reaction. The results show the sensitivity of the cross sections with respect to the hybrid (HYB) and geometry-dependent hybrid (GDH) model calculations using the nucleon mean-free path as a free parameter (the numbers in parentheses are the mean-free-path multipliers). Notice that a good fit to the data can also be obtained by adjusting the mean-free path.

M.G. Mustafa et al

PRC 88

special features:

- -quantum effects are simulated (stochasticity, Pauli blocking, mean field, transmission and reflection)

- -predictive power for (almost) all channels

- -substantiated by nuclear transport theory

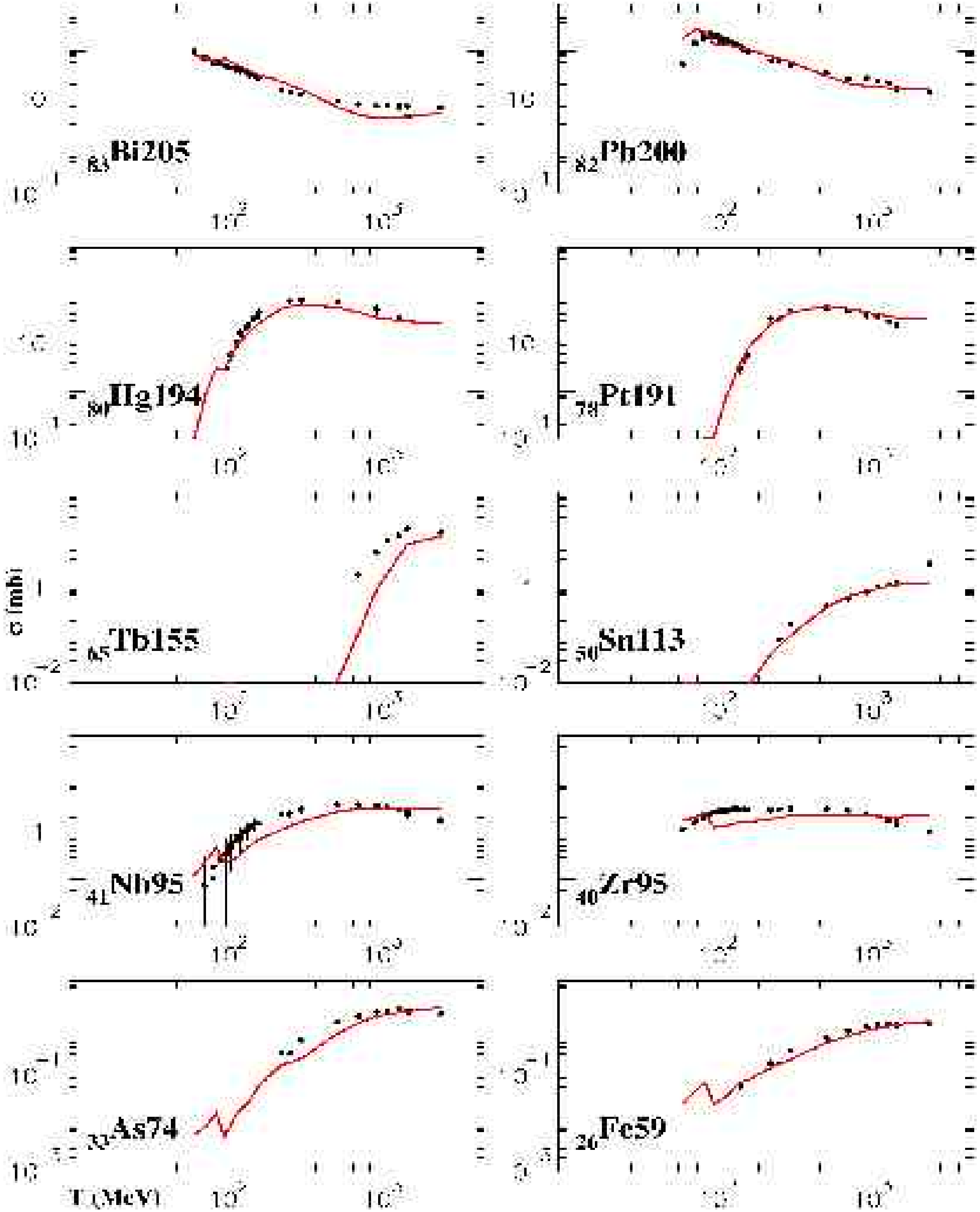

83Bi205
82Pb200
80Hg194
78Pt191
65Tb155
50Sn113
41Nb95
40Zr95
33As74
26Fe59
σ (mb)
T (MeV)

D. TALYS= a code system for E<150 MeV

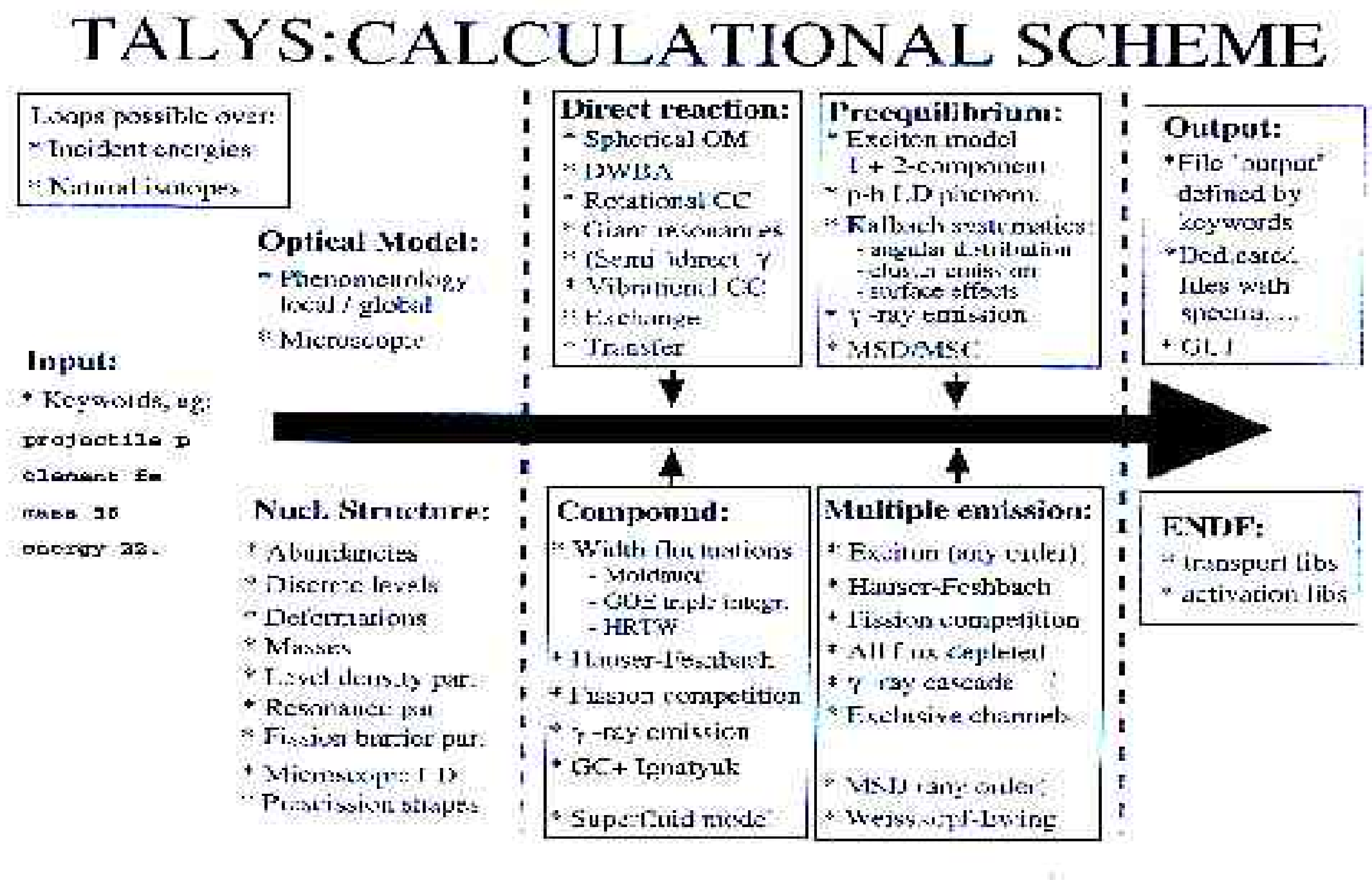

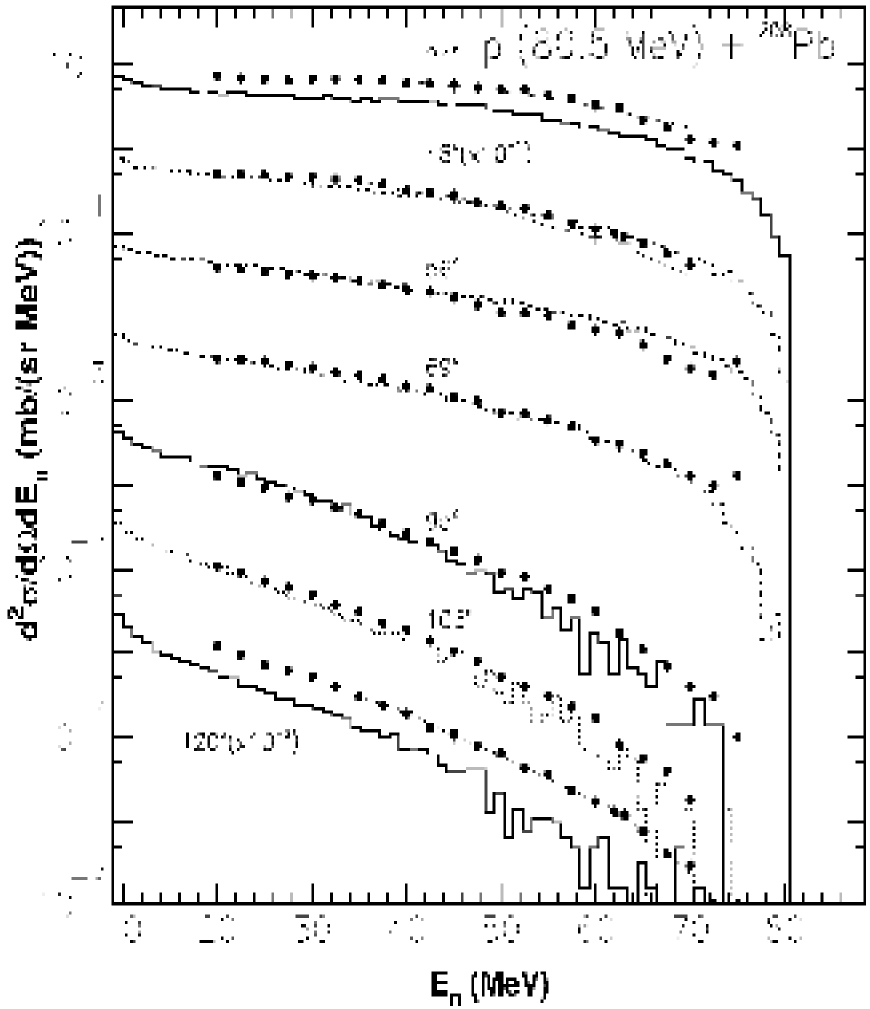
d²σ/dΩdE_n (mb/(sr MeV))
E_n (MeV)

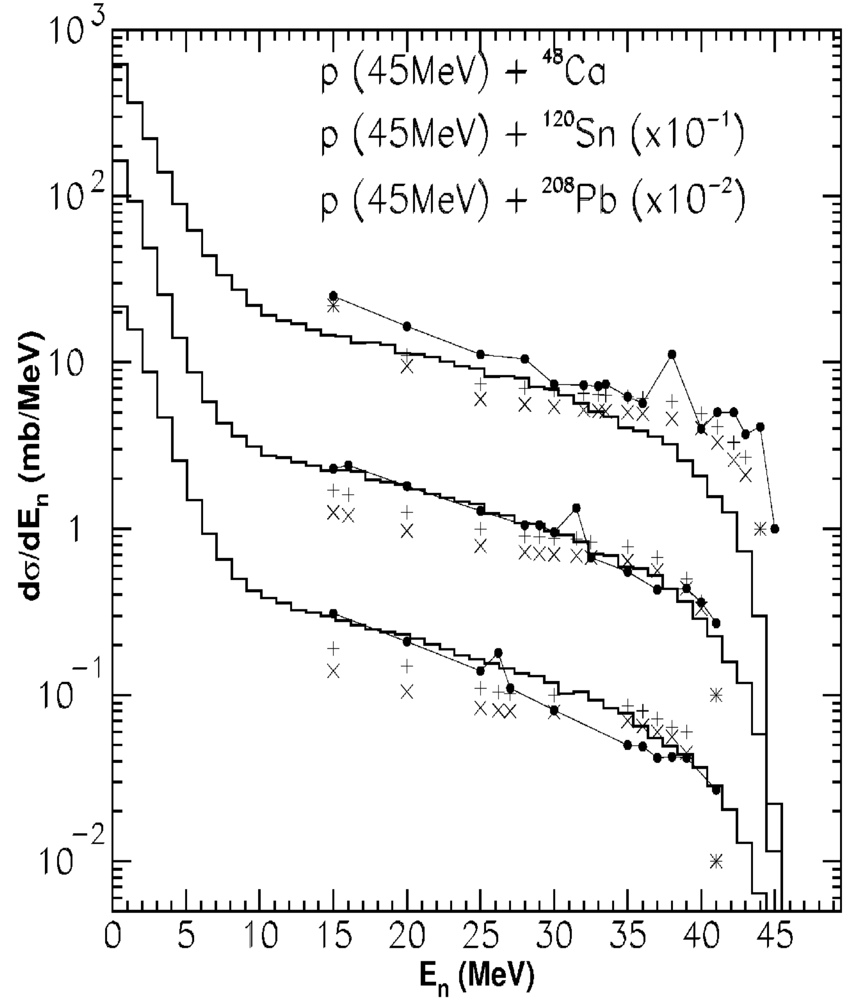
p (45MeV) + ⁴⁸Ca
p (45MeV) + ¹²⁰Sn (x10⁻¹)
p (45MeV) + ²⁰⁸Pb (x10⁻²)
dσ/dE_n (mb/MeV)
E_n (MeV)
10³
10²
10
1
10⁻¹
10⁻²
0
5
10
15
20
25
30
35
40
45

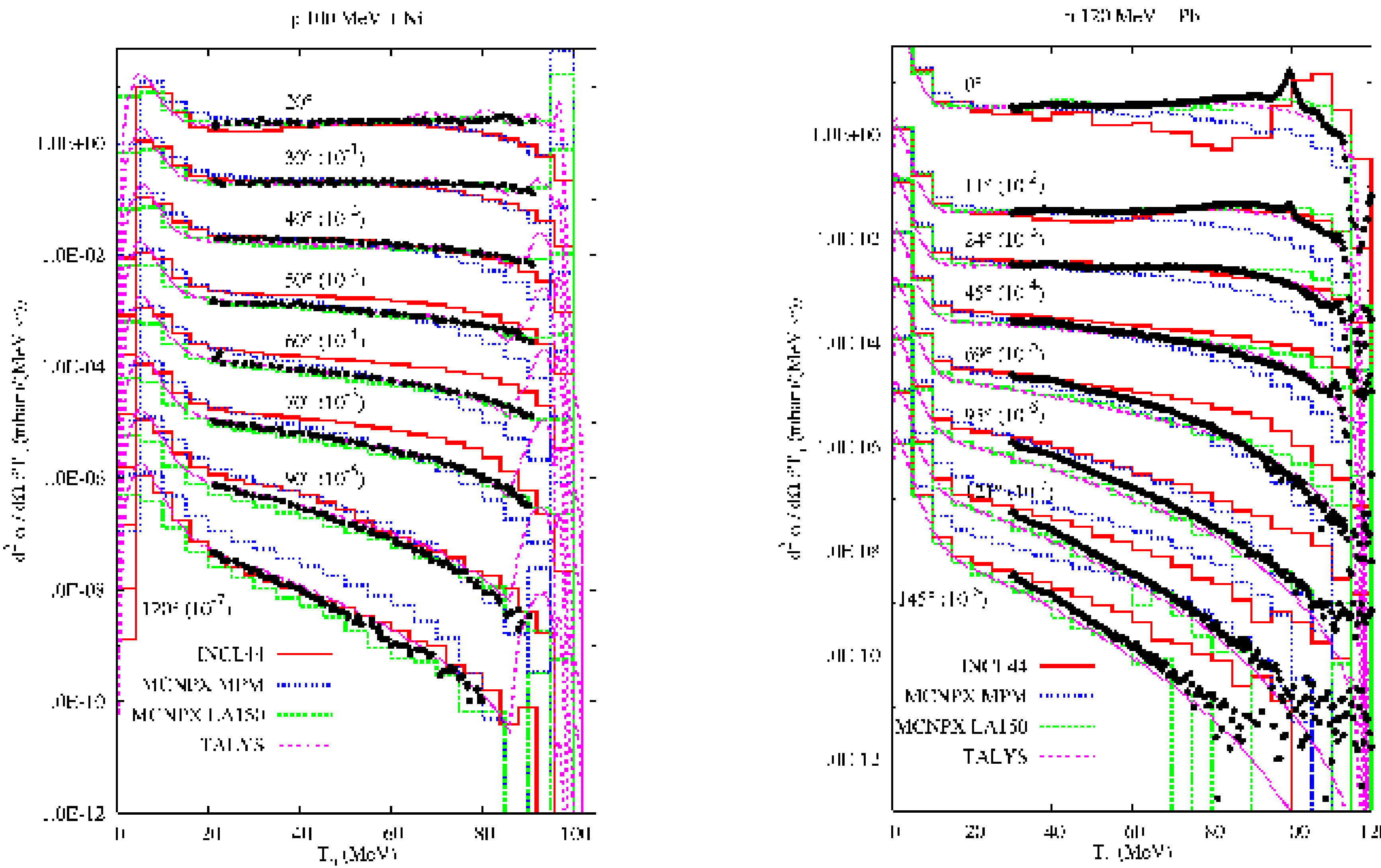

p 100 MeV + Ni
T_p (MeV)
INCL44
MCNPX MPM
MCNPX LA150
TALYS
n 130 MeV + Pb
T_n (MeV)

3. Heavy ion reactions

low and, correspondingly, the expansion of the matter is slow, the shadows left by spectators will not be very pronounced.

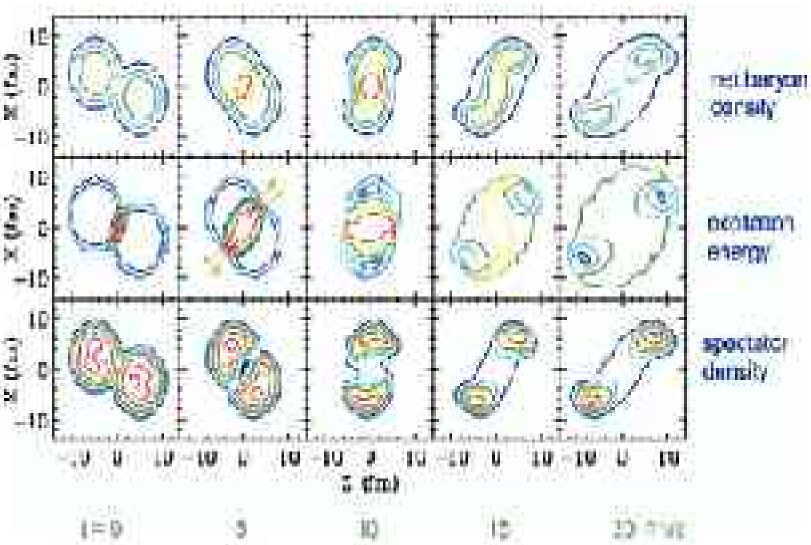

Fig. 5 Reaction-plane contour plots for different quantities in a ^{124}Sn+^{124}Sn reaction at 800 MeV/nucleon and $b=6$fm, from transport simulations by Shi [10].

There are different types of anisotropies in emission that the spectators can produce. Thus, throughout the early stages of a collision, the particles move primarily along the

changing in the course of the reaction.

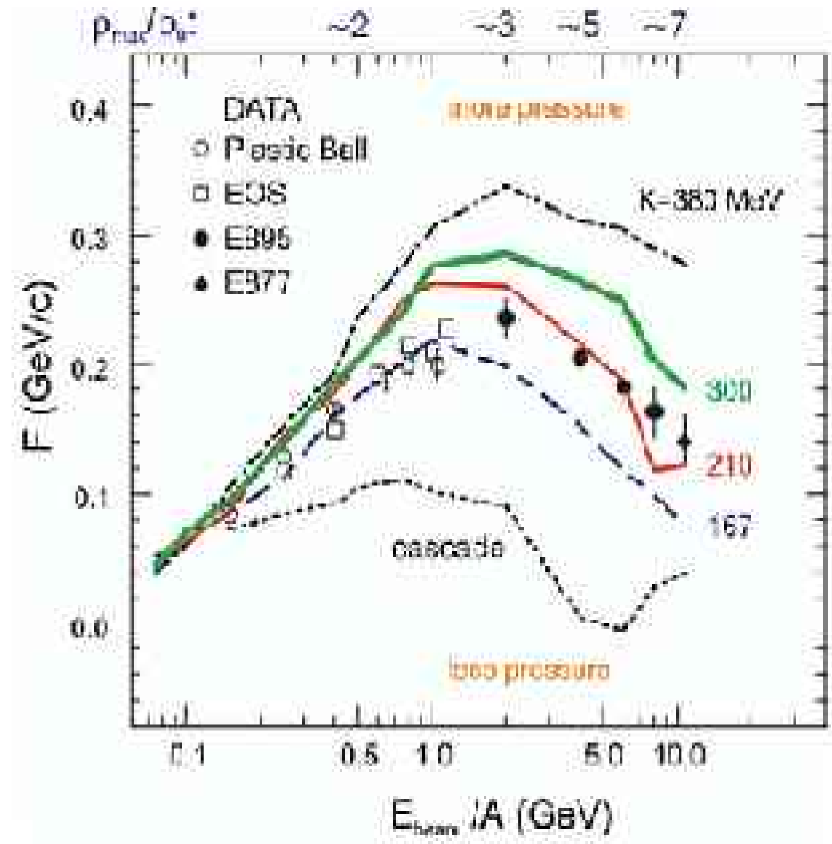

Fig. 6 Sideward flow excitation function for Au+Au. Data and transport calculations are represented, respectively, by symbols and lines [9].

Danielewicz

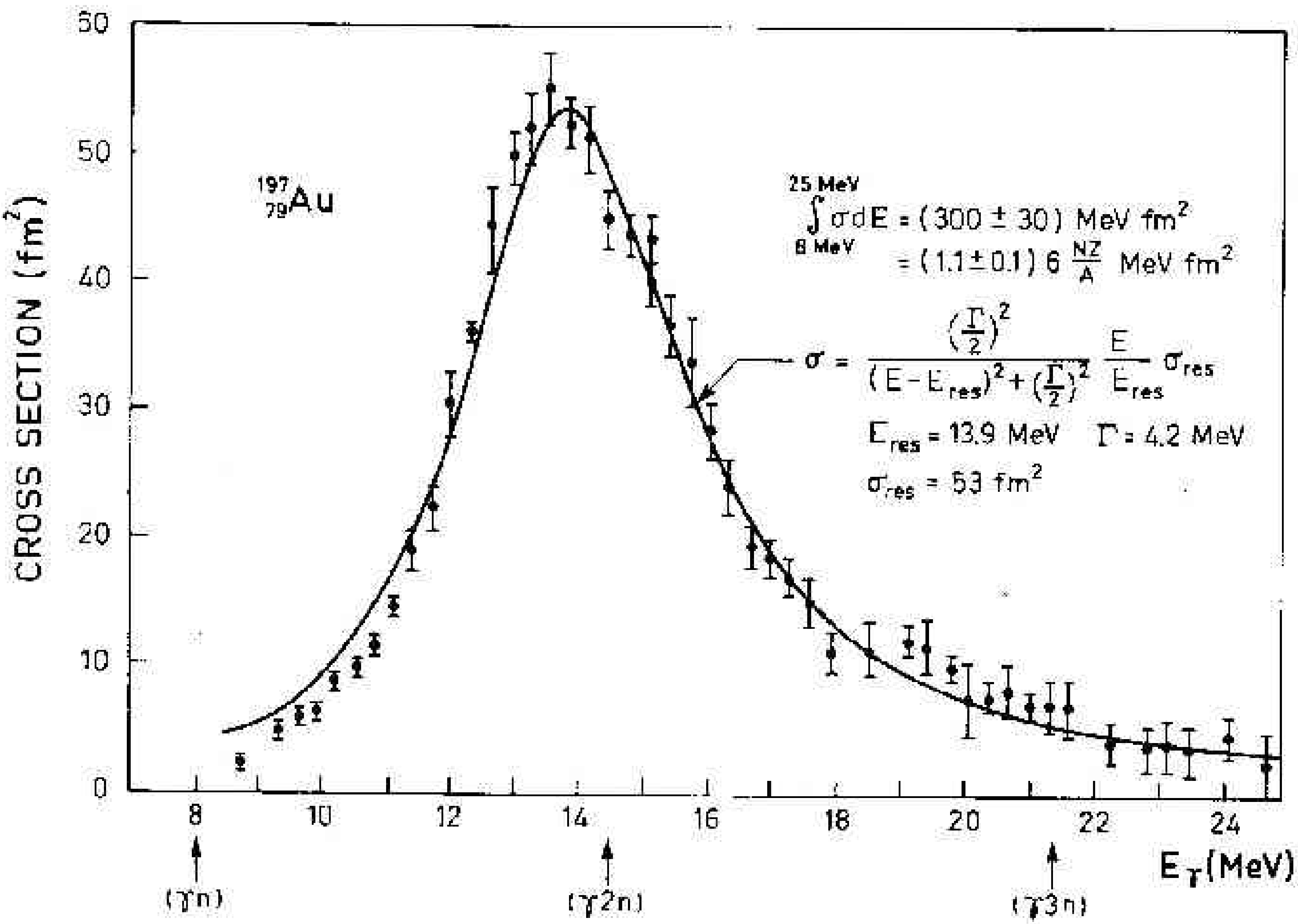

Figure 6-18 Total photoabsorption cross section for ^{197}Au. The experimental data are from S. C. Fultz, R. L. Bramblett, J. T. Caldwell, and N. A. Kerr, *Phys. Rev.* **127**, 1273 (1962). The